Enhanced survival and low proliferation marks multifunctional virus specific memory CD4 T cells

Running title: Heterogenous memory CD4 T cells

Authors
Lotus M Westerhof[1], Jonathan Noonan[2], Kerrie E Hargrave[1], Elizabeth T Chimbayo[1,3], Zhiling Cheng[1,*], Thomas Purnell[1], Mark R Jackson[4], Nicholas Borcherding[5], Megan KL MacLeod[1]

1. School of Infection and Immunity, University of Glasgow, Glasgow, UK
2. Baker Heart and Diabetes Institute & Baker Department of Cardiometabolic Health, University of Melbourne, Melbourne, Australia
3. Malawi Liverpool Wellcome Centre, Blantyre, Malawi
4. School of Cancer Sciences, University of Glasgow, Glasgow, UK
5. Department of Pathology and Immunology, Washington University, St Louis, USA

*Current address: ZC: Pharmacology Research, BeiGene, Shanghai, China.

Corresponding author: Megan KL MacLeod, B515 SGDB, 120 University Place, University of Glasgow, Glasgow, G12 8TA, megan.macleod@glasgow.ac.uk, ORCID: 0000-0003-1843-8580

Abstract

Cytokine production by memory T cells is a key mechanism of T cell mediated protection. However, we have a limited understanding of the survival and secondary responses of memory T cells with cytokine producing capacities. We interrogate antigen-specific CD4 T cells using a mouse influenza A virus infection model. CD4 T cells with the capacity to produce cytokines survive better than non-cytokine+ cells, displaying a low fold contraction and expressing high levels of pro-survival molecules, CD127 and Bcl2. Transcriptomic analysis reveals a heterogenous population of memory CD4 T cells with three clusters of cytokine+ cells. These clusters match flow cytometry data revealing an enhanced survival signature in cells capable of producing multiple cytokines. These multifunctional cells are, however, less likely to proliferate during and following primary and secondary infections. Despite this, multifunctional memory T cells form a substantial fraction of the secondary memory pool, indicating that survival rather than proliferation may dictate which populations survive within the memory pool.

Graphical Abstract

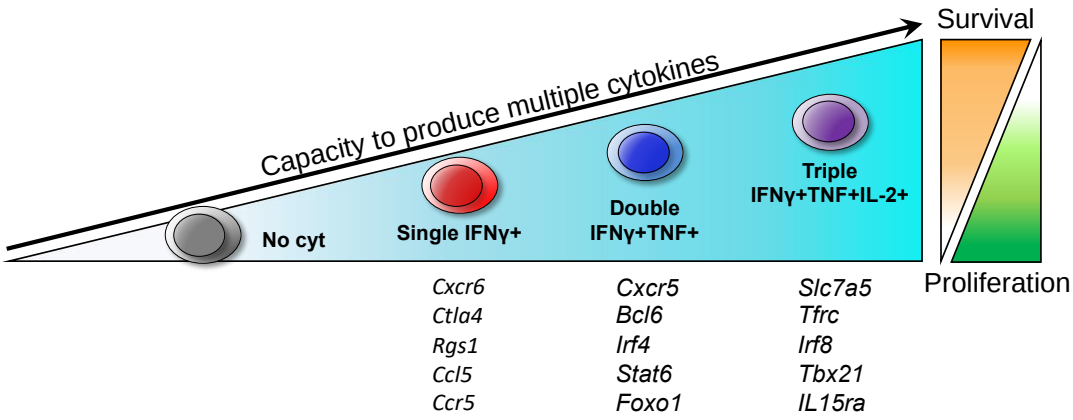

Introduction

Immunological memory protects against repeated infection with a strong and rapid pathogen specific immune response. Cytokine production by memory T cells is often central to this protective response and the presence of T cells that can produce multiple different cytokines is associated with the most effective immune protection (Almeida et al., 2007; Bot et al., 1998; Darrah et al., 2007; Genesca et al., 2007; Kwissa et al., 2007; Lindenstrom et al., 2009; Soudja et al., 2014; Strutt et al., 2010; Teijaro et al., 2010; Turtle et al., 2016). Understanding which memory T cells provide the most effective protection and the signals that generate these cells is a key target towards producing more effective vaccines.

Improving our understanding of T cell memory is particularly important in the context of highly variable infections such as Influenza A Virus (IAV). While neutralising antibodies can prevent IAV infection, the frequent mutations within viral surface proteins makes it difficult for these strain specific antibodies to recognise altered viruses (Webster and Govorkova, 2014). As current IAV vaccines also induce antibodies that target strain specific surface proteins, they induce limited protection against different serotypes. This mechanism of escaping humoral immunity is also observed in other pathogens (Bonsignori et al., 2017; Tao et al., 2021).

We know cytokine producing CD4 and CD8 T cells are key in protection against respiratory viruses, including IAV, at primary infection and upon reinfection with the same or altered viral strains. Importantly, CD4 and CD8 T cells recognise epitopes that are often conserved between IAV strains (Heiny et al., 2007; Wang et al., 2007). The presence of cytokine producing IAV-specific CD4 and CD8 T cells in human peripheral blood correlates with cross-strain protection against symptomatic influenza infection (Hayward et al., 2015; Sridhar et al., 2013; Tsang et al., 2022; Wilkinson et al., 2012). Mechanistic mouse studies have further demonstrated the protective ability of IAV specific CD4 and CD8 T cells, with the inflammatory T-helper (Th1) cytokine, interferon-γ, often key to this response (Bot et al., 1998; Epstein et al., 1998; Liang et al., 1994; McKinstry et al., 2012; Strutt et al., 2010; Teijaro et al., 2010). The cytokines TNF and interleukin (IL-) 2 are also implicated in protection to IAV (Alam et al., 2020; DeBerge et al., 2014). These data support that the most effective memory T cells are those with the capacity to produce cytokines, in particularly multifunctional cells that can produce several different cytokines.

Many studies have demonstrated that tissue resident memory T cells (Trm), predominantly confined to site(s) of infection, can provide rapid protection to re-infection. These studies suggest vaccines should aim to induce Trm cells (Masopust and Soerens, 2019; Sasson et al., 2020). However, heterosubtypic immunity to IAV, mainly mediated by CD4 and CD8 T cells, wanes in the months following infection of mice (Liang et al., 1994). Most studies agree that lung memory CD8 and CD4 T cells decline over time, although recruitment of circulating cells or homeostatic proliferation may maintain these populations to some extent (Ely et al., 2006; Pizzolla et al., 2017; Slutter et al., 2017; Takamura et al., 2019; Zheng and Wakim, 2022). A long-lived protective memory response may, therefore, also be dependent on the generation of memory T cells beyond the pathogen-targeted tissue.

Fundamentally, a deeper understanding of protective memory T cells is required to reveal which memory T cells vaccines should aim to generate. We previously showed that multifunctional CD4 and CD8 T cells increase in predominance from the primary to the memory pool (Westerhof et al., 2019). Building on this finding, we have now characterised the generation, survival, and function of these memory T cells following IAV infection in multiple tissues.

We define that a low fold contraction and a low level of proliferation by multi-functional T cells defines their increased predominance in the memory pool. Moreover, focusing on the CD4 compartment, we show T cells producing multiple cytokines demonstrate a strong pro-survival

transcriptional signature. However, despite this pro-survival signature, multifunctional T cells proliferated poorly during a secondary IAV challenge *in vivo*, in contrast to single IFNγ+ T cells. By comparing memory CD4 T cells that do or do not have the capacity to produce cytokines, we reveal that cytokine producing T cells have an enhanced capacity to survive into the memory pool. Consequently, our study challenges the memory T cell paradigm that less differentiated central memory T cells have enhanced survival compared to more differentiated effector memory T cells (Catron et al., 2006; Mueller et al., 2013; Nguyen et al., 2019; Wherry et al., 2003).

Results

IAV specific CD4 and CD8 T cells can be tracked using MHC tetramers and via ex vivo cytokine responses

We used MHC I and MHC II tetramers (tet) containing immunodominant IAV nucleoprotein (NP) peptides, (NP_{368-74} and $NP_{311-325}$) to identify IAV-specific T cells longitudinally following IAV infection, Figure 1A-B; gating shown in Supplementary Figure 1. These same peptides were used to separately activate cells from the same mice *ex vivo* to examine the anti-IAV T cell cytokine responses, Figure 1B, as optimal dual staining of MHC tetramers and cytokine was not possible. IAV infected animals were injected with fluorescently labelled anti-CD45 shortly before euthanasia to label cells in the blood; lung IAV-specific T cells that are CD45iv negative are likely Trm cells (Son et al., 2021).

In the lymphoid organs, the majority of MHC tet+ and cytokine+ CD4 and CD8 T cells were negative for CD45iv, Figure 1C. The majority of lung IAV specific CD4 T cells were also not labelled with the i.v. injected anti-CD45 at any timepoints. In comparison, around 50-60% of the MHCI tet+ CD8 T cells were CD45iv+ at all time points and the proportion of labelled CD8 IAV specific IFN-γ+ and TNF+ T cells in the lung increased after day 9.

We examined the phenotype of the MHC tet+ T cells comparing cells in the spleen, dLN and lung across the three time points, Figure 1D and Supplementary Figure 1C-D. There were too few MHCII tet+ CD45+ lung CD4 T cells at memory time points to analyse, but we have included data on CD45iv+ CD8 T cells.

As expected, PD1 was expressed on activated T cells and declined after day 9 on CD4 and CD8 T cells in T cells from all organs. However, MHC tet+ CD45iv negative CD4 and CD8 T cells in the lung continued to express higher levels than T cells from the lymphoid organs.

The cell surface markers CD69 and CD103 are associated with Trm cells (Casey et al., 2012; Masopust and Soerens, 2019; Sasson et al., 2020). Expression of these molecules increased on CD8 MHCI tet+ cells in the lymphoid organs and CD45iv negative lung cells after day 9. However, very few CD4 MHCII tet+ cells expressed these markers.

While at day 9 some CD4 MHCII tet+ cells in the lung expressed CX3CR1, only a small minority of memory cells expressed this chemokine receptor. CX3CR1 was expressed by CD8 MHCI tet+ cells, most prominently in the spleen and on lung CD45iv+ cells suggesting that these are circulating effector memory cells (Gerlach et al., 2016).

The phenotype of the lung CD45iv+ MHCI tet+ CD8 T cells more closely resembled the cells in the spleen rather than the CD45iv negative cells in the lung. The exception was in expression of CD69. While spleen MHCI tet+ CD8 T cells increase expression of CD69 across the time course, the circulating lung MHCI tet+ CD8 T cells remained low.

T cells with the capacity to produce cytokines are more likely to enter the memory pool than non-cytokine+ T cells

We examined the decline of T cells detected with either MHC tetramers or IFNγ production following NP peptide restimulation. As the MHC tetramers detect NP specific T cells regardless of their ability to produce cytokines, differences in the dynamics of their decline are suggestive of differences between cytokine+ and negative populations. MHCII tet+ CD4 T cells declined in the spleen and lung between day 9 and 30 following infection; in the lymph node there was a significant reduction in cells by day 70, Figure 2A. In contrast, IFNγ+ CD4 T cells did not drop significantly until day 70 in the spleen and lung and did not decline at all in the dLN. These data suggest that MHCII-NP specific CD4 T cells with the capacity to produce IFNγ are more stably maintained than cells of the same specificity that cannot produce IFNγ.

A somewhat similar picture was observed in the CD8 T cells, Figure 2B. In the spleen and lymph node, MHCI tet+ CD8 T cells dropped only slightly and this was significant only by day 70 in the lymph node. In the lung these cells had declined by day 30. IFNγ+ CD8 T cells did not decline at either memory timepoint in the lymphoid organs but did show a significant decline by day 30 in the lung.

We also examined IL-2+ and TNF+ CD4 and CD8 T cells and found a similar pattern as for IFNγ+ T cells with decline in cytokine+ cells most obvious in the lung and only significantly reduced at day 70, Figure 2C-D. Interestingly, IL-2+ CD8 T cells showed a trend to increase in the spleen from day 9 to day 70, and this was a significant increase for TNF+ CD8 T cells. While TNF+ cells mainly mirrored IFNγ+ cells in the lung, IL-2+ CD8 T cells in the lung remained stable across all three timepoints, although the number of these cells was low.

Collectively, these data suggest that NP-specific CD4 and CD8 T cells with the capacity to produce cytokines are more stable between day 9 and 30 than the total NP memory T cell pool. This suggests that T cells with the capacity to produce cytokines display enhanced survival compared to those that cannot produce cytokines. Interestingly, for CD4 T cells, these changes were accompanied by an increase in sensitivity to peptide by the cytokine+ cells, with memory CD4 T cells producing TNF and IL-2 at lower peptide concentrations than cells at day 9. In contrast, primary and memory CD8 T cell cytokine production was unaffected by the peptide dose, Supplementary Figure 2.

Memory T cells with the capacity to produce cytokines express higher levels of pro-survival molecules than T cells that cannot produce cytokines

To compare the phenotype and function of cytokine+ and negative IAV specific CD4 T cells, we took advantage of a reporter mouse we have developed (Gray et al., 2021). In these triple transgenic mice, activated T cells express rtTA, which, when bound to doxycycline, activates the tet-ON promoter, driving Cre expression which leads to permanent EYFP production at the ROSA locus. Infection with IAV induced a substantial population of EYFP+ CD4 T cells when triple transgenic mice were fed a doxycycline+ diet during the initial infection, Supplementary Figure 3. This model greatly increases the number of responding T cells we can identify and enables identification of cytokine+ and negative EYFP+ cells within the same sample.

As the EYFP+ cells are likely to respond to an array of IAV antigens, we used bmDCs cultured with a sonicated IAV antigen preparation to restimulate the T cells *ex vivo* for cytokine analysis (Westerhof et al., 2019). The expression of the pro-survival molecules CD127 and Bcl2 was examined in EYFP+ cytokine negative CD4 T cells and those expressing IFNγ, IL-2 and TNF following *ex vivo* restimulation, Figure 3A. The cytokine+ EYFP+ T cells expressed higher levels of both molecules compared to cytokine negative cells, Figure 3B-C. These data are

consistent with the hypothesis that CD4 T cells with the capacity to produce cytokines have an enhanced survival capacity compared to non-cytokine+ T cells.

T cells that can produce multiple cytokines are more persistent than those that only have the capacity to produce IFNγ

To investigate the cytokine+ T cells in more detail, we separated these into single IFNγ+, double IFNγ+ TNF+ or IL-2+ cells, or triple cytokine+ cells capable of making all cytokines. Triple cytokine+ CD4 T cells detected following *ex vivo* culture with IAV-Ag+ bmDCs did not decline in any of the organs between days 9 and 30, Figure 4A. All other populations declined significantly in at least one of the organs examined although cells in the lymph node had limited decline regardless of which population was examined. A similar pattern of results was found for CD4 cytokine+ T cells reactivated with NP peptide, although in the spleen the single IFNγ+ were more stable, Figure 4B. These data suggest there may be some differences between CD4 T cells responding to this immunodominant peptide compared to the broader IAV-specific CD4 T cell pool.

There were no significant declines in the numbers of cytokine+ CD8 T cells detected following incubation with antigen or peptide loaded bmDCs, Figure 4C-D. However, in the lung, while triple cytokine+ CD8 T cells were clearly stable, the single IFNγ+ and double IFNγ+TNF+ cells displayed non-significant drops. Interestingly, triple cytokine+ CD8 T cells specific for NP peptide tended to increase from day 9 to day 30, suggesting potential conversion from another cytokine+ or a cytokine negative population.

CD4 triple cytokine+ T cells express more cytokines at an individual cell level

Previous studies have demonstrated that multifunctional T cells produce more IFNγ on a per cell basis than single IFNγ+ T cells (Almeida et al., 2007; Darrah et al., 2007; Lindenstrom et al., 2009). We confirm that triple cytokine+ CD4 T cells in our experiments expressed more IFNγ at day 9 and day 30, Figure 5. Moreover, by gating on total IL-2+ or TNF+ T cells, we found that triple cytokine+ CD4 T cells also expressed more of these cytokines on a per cell basis than single IL-2+ or TNF+ cells respectively, although lung IL-2+ CD4 T cells do not display this pattern. Interestingly double cytokine+ CD4 T cells mainly displayed an intermediate phenotype with a tendency to produce more of the cytokine than single producers but less than triple+ T cells. We focused on CD4 T cells for these analyses given the low number of IL-2+ CD8 T cells.

Single IFNγ+ CD4 and CD8 T cells are more likely to be in cell cycle than multifunctional T cells

We examined whether increased proliferation by T cells with the capacity to produce multiple cytokines could explain the improved persistence of these cells. For these analyses, we focussed on T cells detected following *ex vivo* reactivation with bmDCs presenting IAV antigens as these provided more robust populations than following peptide-restimulation. The numbers of IFNγ/IL-2 double+ T cells were low and therefore were not included in the analysis.

In the dLN at day 9, over 20% of the CD4 and 30% of the CD8 cytokine+ T cells were Ki67+. In contrast, in the spleen and lung, less than 15% of the CD4 and 25% or less of CD8 cytokine+ cells were Ki67+, Figure 6A-B. As expected, the percentages of T cells that were Ki67+ decreased from day 9 to day 30 and very few Ki67+ cells could be detected on day 70.

We gated on the IFNγ+ Ki67+ cells to examine whether these cells were producing one or more of the cytokines. We hypothesised that triple cytokine+ cells may be more likely to proliferate to maintain their numbers in the memory pool. In contrast, we found the opposite

result: IFNγ single+ CD4 and CD8 T cells were more likely to be in cell cycle compared to triple+ cells at both day 9 and 30, Figure 6C-D. These data rule out the hypothesis that triple cytokine+ cells increase proportionally in the memory pool compared to the primary pool because they proliferate more than single IFNγ+ cells. The data do suggest that the single IFNγ+ T cells may be exposed to remaining antigen that continues to drive their activation and proliferation (Jelley-Gibbs et al., 2005; Zammit et al., 2006).

In support of this, in separate experiments we found that CD4+ single IFNγ+ T cells in the spleen and lung expressed the highest levels of ICOS and this was also the case for PD1 in the lung, Figure 6E-F; there were too few cells in the dLN for these analyses. These data support our hypothesis that the single IFNγ+ T cells may be more activated than other cytokine+ populations and that potentially these cells are in contact with persisting antigen (Jelley-Gibbs et al., 2005; Zammit et al., 2006).

Multifunctional and single IFNγ+ cells express similar levels of CD127 and Bcl2 but single IFNγ+ T cells have a more activated phenotype

The triple cytokine+ T cells may display greater persistence than the single IFNγ+ T cells because they express higher levels of survival molecules. To address this, we compared the expression of CD127 and Bcl2 on single, double and triple cytokine+ cells. There were too few triple+ CD8 T cells in any organ and too few cytokine+ cells in the dLN to compare the MFI of the different populations. Therefore, we focussed on cytokine producing CD4 T cells in the spleen and lung.

At day 30 post-infection, we found that double and triple cytokine+ CD4 T cells in the spleen had higher expression of CD127 and triple+ cells in the spleen expressed more Bcl2 than double IFNγ+TNF+ cells, Figure 7 A-B. While there was a trend for the triple cytokine+ cells in the lung to express higher levels of CD127 and Bcl2, this did not reach significance. These data suggest that the differences in these two pro-survival molecules may not be sufficient to explain the altered survival in lung cytokine+ memory T cells.

Single cell RNAseq analysis reveals a pro-survival gene signature in triple cytokine+ memory CD4 T cells

To obtain a more detailed understanding of differences between the cytokine positive and negative memory T cell populations, we performed single-cell gene transcription analysis. CD4 T cells from the spleens and lungs from TRACE mice infected with IAV 40 days previously were activated with IAV-Ag DCs for 4 hours to reveal those with the capacity to produce cytokines. CD45iv negative, EYFP+ CD44^{hi} cells from the spleen and lung and control naïve (CD44^{lo}/EYFP negative) spleen cells were FACS sorted and gene expression examined via BD-Rhapsody single-cell transcriptomic analysis using the Immune Response Targeted panel for mouse.

Initial clustering produced 19 different clusters, including 8 naïve/central memory clusters, 10 memory clusters and one Treg cluster, Supplementary Figure 4A. To focus on the differences between the memory clusters, we reduced the complexity of the naïve/CM population into a single population, Figure 8A; all clusters remained transcriptionally distinct, Supplemental Figure 4B; Supplementary Table 1. Of the 10 memory clusters, 7 expressed little to no *Ifng*, *Tnf or Il2*, Supplemental Figure 4C. Cells from all clusters were found in both the spleen and lung, with the spleen contributing most cells in all but one cluster. The exception was the single+ cluster expressing *Ifng* but not *Tnf* or *Il2*, which was predominantly derived from the lung, Figure 8A & Supplementary Figure 4D.

We first focussed on the transcriptional signatures of the three cytokine producing clusters: single+ (*Ifng*) double+ (*Ifng* & *Tnf*), and triple+ (*Ifng, Tnf* & *Il2*) cells, Figure 8B & Supplementary Table 1. The single+ CD4 T cells expressed the highest levels of *Icos* and *Pdcd1* (PD1), confirming our flow analysis. These cells also expressed other transcripts implicated in T cell activation including *Ctla4*, *Tnfrsf9* (41BB), and *Ccl5*. High expression of *Cxcr6* and *Rgs1* may reflect that many of these were isolated from the lung (Kumar et al., 2017) and expression of *Xbp1* tallies with the proliferative ability of these cells (Pramanik et al., 2018).

Genes uniquely upregulated in the double+ cells indicated a Tfh-like phenotype, supported by the expression of *Cxcr5*, *Bcl6, Irf4* (Crotty, 2019; Krishnamoorthy et al., 2017) and *Foxo1* (Stone et al., 2015), suggesting these cells may be particularly important in supporting the antibody response in either the spleen or lung (MacLean et al., 2022; Swarnalekha et al., 2021).

Triple+ cells were uniquely enriched for *Il2* and, while the single+ and double+ clusters clearly expressed *Ifng* +/- *Tnf*, these transcripts were only significantly enriched (versus all other cells) within the triple+ cluster. The high expression of these three cytokine transcripts within the triple+ cells clearly reflected our protein-based flow cytometry data. In addition, Triple+ cells were also enriched for genes such as*Tnfsf14* (LIGHT), *Tbx21* (T-bet), *Il2ra* and *Irf8*.

We also observed genes commonly enriched across some or all cytokine+ clusters. For example, the double and triple cytokine+ cells had overlapping expression of several genes reflective of T cell activation and differentiation including *Cd69*, *Icam1*, *Fyn* and *Stat5a*. Strikingly, the double and triple cytokine+ cells expressed high levels of the transcription factor *Myc* and we confirmed increased Myc protein expression in triple+ cells by flow cytometry, Figure 8C and Supplementary Figure 4E.

Myc is a key regulator of T cell metabolism downstream of activation and may confer both proliferative and/or survival advantages for these cells (Marchingo et al., 2020). In addition to being the highest expressors of *Myc,* Triple+ cells were also enriched for *Myc* pathway associated transcripts, expressing the highest levels of *Ybx3* (Marchingo et al., 2020) and being uniquely enriched for *Tfrc* (CD71) and *Slc7a5* within the cytokine positive populations. Collectively, these data suggest that these T cells have a distinct metabolic profile compared to the other memory populations.

Interestingly, the different clusters of memory T cells expressed varying combinations of chemokine receptors suggesting that they may be located in distinct regions of the lung and spleen and/or respond distinctly following re-infection, Figure 8D. Finally, the triple cytokine+ memory CD4 T cells expressed high levels of molecules associated with survival, Figure 8E. These included Bcl2 family members (*Bcl2a1a* (Flores-Fernandez et al., 2021; Metais et al., 2012) and *Bcl2l1*(Bclx) (Wang et al., 2012)), receptors for pro-survival cytokines (*Il2ra*, *Il15ra* (Leonard et al., 2019)) and costimulatory molecules (*Tnfrsf4* (OX40), *Tnfsf8* (CD30L) associated with T cell survival (Croft et al., 2009; Nishimura et al., 2005; Tang et al., 2008). Surprisingly, the cytokine+ cells expressed low levels of *Il7r* (CD127) which is in contrast to our flow cytometry data, Supplementary Figure 4B. This may reflect that gene transcription does not always relate to protein expression (Buccitelli and Selbach, 2020).

TCR clones are found in multiple memory T cell clusters but are not shared between different animals

We used CDR3 sequencing of the T cells' TCRs to address whether clones were restricted to particular memory T cell clusters within the scRNAseq data. We found expanded clones within each of the memory populations, with the relative absence of these in the naïve/CM and regulatory populations, Figure 9A-B. Few expanded clones appeared cluster specific, with

most represented across multiple clusters, Figure 9C-D. These data suggest that TCR CDR3 sequence does not dictate T cell fate. Finally, analysis of expanded clonotypes derived from each animal demonstrated little evidence of public T cell clones, Figure 9E.

Single IFNγ+ T cells dominate the proliferative response during re-infection

Our data above and the relationship between T cell multifunctionality, persistence into the memory pool, and protection from disease suggest that triple cytokine+ T cells should dominate a secondary response to IAV (Almeida et al., 2007; Darrah et al., 2007; Genesca et al., 2007; Kwissa et al., 2007; Lindenstrom et al., 2009; Westerhof et al., 2019). In particular, the high expression of Myc by the triple and double cytokine+ cells suggested these cells would respond and proliferate robustly following reactivation (Marchingo et al., 2020).

To test this, we re-infected IAV-memory mice with a distinct strain of IAV, X31, which has different surface proteins to IAV-WSN. This ensure that neutralising antibody to the WSN-IAV surface proteins does not prevent infection and T cell reactivation. In this model, T cell responses are associated with immune protection (Liang et al., 1994). As expected, IAV-memory mice were protected from weight loss following infection with X31-IAV, Supplementary Figure 5A.

We analysed cytokine production by memory T cells before and 5 days after re-infection. The numbers of cytokine+ (IFNγ, IL-2, TNF) CD4 and CD8 T cells increased only slightly following re-infection, Fig 8A-B, Supplementary Figure 5B-C. Re-infection also led to an increase in the percentages of cytokine+ cells that were in cell cycle, most notably in cells in the spleen and dLN, Figure 8C-D, Supplementary Figure 5D-E. This was the case for both CD4 and CD8 T cells and regardless of which cytokine we examined; we did not analyse IL-2+ CD8 T cells as the numbers were too low. Most of the cytokine+ T cells were not, however, positive for Ki67, reflecting the low increase in cell number.

We next examined whether the IFNγ+ Ki67+ T cells were skewed towards single or multifunctional T cells, Figure 8E-F. For CD4 T cells in the dLN and lung, single IFNγ+ and double IFNγ+TNF+ cells had higher expression of Ki67 than triple cytokine+ cells. We saw a similar pattern in CD8 T cells in the spleen, dLN and lung with triple cytokine+ least likely to be Ki67+.

The low levels of Ki67 in triple cytokine+ cells may suggest that these cells would be less prevalent following reactivation and that single or double positive T cells may become a more prominent population. This was not the case. The percentages of IFNγ+ cells that were also expressing IL-2 and/or TNF were the same before and at day 5, Supplementary Figure 5 F and day 35 following re-infection, Figure 8G-H. Moreover, mice given a primary infection with X31 had similar proportions of single, double and triple+ cells at day 35; too few cells were present in the primary infected mice at day 5 to analyse.

These data suggest that while CD4 triple cytokine+ T cells may be less likely to proliferate following reactivation, they are equally, or potentially better, equipped to survive into the secondary memory pool. In contrast, the single and double cytokine+ T cells that do proliferate following re-infection may be more likely to undergo apoptosis. Together these data suggest that these cytokine+ cell populations have distinct roles to perform during secondary response.

Discussion

Here we reveal extensive heterogeneity within the memory CD4 T cell pool in lymphoid organs and the lung. Transcriptomic heterogeneity was clearly present within cells with the capacity to produce IFNγ, the key cytokine most associated with protection from IAV (Bot et al., 1998; Hayward et al., 2015; Soudja et al., 2014; Sridhar et al., 2013; Strutt et al., 2010; Teijaro et al., 2010; Tsang et al., 2022; Wilkinson et al., 2012). Importantly, our data suggest that heterogeneity within the memory pool also covers a spectrum of cells that do not fit into our current memory T cell paradigms that were first defined based on cell migration patterns rather than functional capacity.

Using various approaches to track IAV specific CD4 T cells we have made a number of key novel findings. First, our data show that the capacity to produce cytokines marks T cells with an enhanced ability to survive into the memory pool. Identification of the factors and cell types that promote cytokine+ cells could define how we could increase the size of the memory T cell pool following vaccination.

Second, within the cytokine+ fraction of the memory pool, we consistently identified three populations based on the capacity to produce one or more of IFNγ+, IL-2 and TNF. These three populations expressed distinct chemokine receptors, different levels and types of markers of T cell activation, and pro-survival molecules. These data suggest that these cells may have defined anatomical niches perhaps as a driver or result of their differentiation. These differences may impact on the cells' survival and, importantly, their responses to reinfection. Alternatively, the populations could be distinct temporal states with cells oscillating between these clusters depending on recent interactions with other cell types and/or soluble molecules produced by these cells.

A caveat of our model is that detection of the cytokine producing cells involves a short *ex vivo* reactivation stage. We therefore cannot know whether the expression of these molecules is altered during the reactivation. Our previous data did, however, demonstrate that single, double, and triple cytokine+ populations could be identified as early as 2 hours after re-activation, suggesting that these three populations are reflective of *in vivo* CD4 T cells with distinct phenotypes and functions (Westerhof et al., 2019).

Double IFNγ+/TNF+ CD4 memory T cells often displayed an intermediate phenotype between triple cytokine+ cells and single IFNγ+ cells, for example in expression of Ki67, PD1, ICOS, Myc and the cytokines themselves. We think it is an over-simplification to consider these cells an intermediatory phase between single and triple cytokine+ cells as the double cytokine+ cells had a distinct transcriptional signature. Notably, the transcriptional signature of the double IFNγ+/TNF+ has some overlap with Tfh cells and the recently described T resident helper cells, including expression of *Cxcr5* and *Bcl6* (Son et al., 2021; Swarnalekha et al., 2021). Resident Tfh and memory-Tfh like cells have been shown to differentiate into multiple different effector subsets upon re-activation *in vivo* suggesting these cells retain a level of plasticity (Kunzli et al., 2020; Swarnalekha et al., 2021). To test definitively the relationships between the three cytokine populations, comprehensive longitudinal lineage tracing approaches would be required.

We were surprised that the double and triple cytokine+ CD4 memory T cells did not dominate the secondary response to IAV. These cells expressed high level of transcripts for *Myc*, *Slc7a5* and the transferrin receptor, suggesting that they are poised to respond and proliferate following TCR activation (Marchingo et al., 2020). We cannot exclude that memory triple or double cytokine+ CD4 T cells differentiate into single IFNγ+ during the re-infection. We think this is unlikely given the small changes in cell number and the stability of proportions of triple/double/single cytokine+ cells at days 5 and 30 following IAV re-infection. While there has

been limited analysis of tertiary memory CD4 T cells, Bresser *et al* recently demonstrated that central memory CD8 T cell that have previously undergone the fewest rounds of division and have low expression of 'effector cell' genes dominate the secondary response (Bresser et al., 2022). In contrast, Wirth *et al* found that CD8 T cells can show increasing complexity following subsequent activation suggesting a contribution from multiple memory population to the tertiary pool (Wirth et al., 2010).

We identified IAV specific CD4 T cells using methods that restrict the population to a single immunodominant epitope or to T cells responding to numerous IAV epitopes. Our results on T cell survival are largely consistent between these methods suggesting that TCR specificity does not influence T cell survival into the memory pool. This conclusion is reinforced by finding the same TCR clones in several of the clusters within the single-cell RNAseq dataset. We suggest that environment is more likely, therefore, to dictate cell fate, than signals through the TCR.

We have analysed IAV specific CD4 and CD8 T cells in the same animals highlighting some key differences between these cell types. Most notably, cytokine+ CD8 T cells display a very limited decline in lymphoid organs with TNF+ memory CD8 T cells increasing over time. This reflects similar findings in LCMV infected mice in which the numbers of CD8 memory T cells able to produce cytokine following peptide stimulation remained stable for over 900 days while memory CD4 T cells declined (Homann et al., 2001). A second distinction in our study was revealed by examining sensitivity to the immunodominant peptides. While CD8 T cells produced a maximal cytokine response regardless of peptide dose, CD4 T cells produced less cytokine at lower peptide doses. It will be important to extend these data, examining T cells responding to other epitopes.

We did find consistent patterns of proliferation in IAV specific CD4 and CD8 T cells. Single IFNγ+ CD4 and CD8 T cells were more likely to be Ki67+ at primary, memory and recall timepoints compared to triple or double cytokine+ T cells. These data suggest that the link between proliferation capacity and multi-functionality is common to both CD4 and CD8 T cells. Understanding the molecular mechanisms that underlie this link could, therefore, reveal pathways that can be manipulated to enhance both the CD4 and CD8 T cell responses in the context of infectious disease and cancer or limit such responses in autoimmune pathologies.

Materials and Methods

Study design

The aim of this study was to understand how cytokine production by memory CD4 and CD8 T cells changes over time and following a challenge re-infection. We used an influenza virus infection model in wildtype and reporter mice and tracked responding cells using MHC tetramers, cytokine assays and the reporter system in the TRACE transgenic mice (Gray et al., 2021). A description of the experimental parameters, samples sizes, any samples that were excluded, and the statistical analysis are described in each figure legend. No specified randomisation was conducted. Analysis of data was conducted in an unbiased manner.

Animals

10 week old female C57BL/6 mice were purchased from Envigo (UK). TRACE male and female and female C57BL/6 mice were maintained at the University of Glasgow under specific pathogen free conditions in accordance with UK home office regulations (Project Licenses P2F28B003 and PP1902420) and as approved by the local ethics committee. TRACE mice have been described previously (Gray et al., 2021).

Infections

IAV was prepared and titered in MDCK cells. 10-14 week old female C57BL/6 and male and female TRACE mice were briefly anesthetised using inhaled isoflurane and infected with 150-200 plaque forming units of IAV strain WSN in 20μl of PBS intranasally (i.n.). These mice are between 18-25g at the start of the experiment. Infected mice were rechallenged with 100PFU of X31. Infected mice were weighed daily for 14 days post-infection. Any animals that lost more than 20% of their starting weight were humanely euthanised. TRACE mice were given Dox+ chow (Envigo) for a total of 10 days starting two days prior to infection.

Tissue preparation

Mice were injected intravenously (i.v.) with 1μg anti-CD45 (30F11, either labelled with Alexa 488 or PE, both from ThermoFisher) 3 minutes before being euthanized by cervical dislocation. Spleen and mediastinal lymph nodes were processed by mechanical disruption. Single cell suspensions of lungs were prepared by digestion with 1mg/ml collagenase and 30μg/ml DNAse (Sigma) for 40 minutes at 37°C in a shaking incubator followed by mechanical disruption. Red blood cells were lysed from spleen and lungs using lysis buffer (ThermoFisher).

Ex vivo reactivation for cytokine

Bone marrow DCs were prepared as described(Inaba et al., 1992). Briefly, bone marrow cells were flushed from the tibias and femurs of female C57BL/6 mice and red blood cells removed. Cells were cultured in complete RPMI (RPMI with 10% foetal calf serum, 100μg/ml penicillin-streptomycin and 2mM L-glutamine) at 37°C 5% CO_2 in the presence of GM-CSF (prepared from X-63 supernatant (Stoiber et al., 2001)) with media supplemented on day 2 and replaced on day 5. On day 7, DCs were harvested, incubated overnight with IAV antigen (MOI of 0.3) prepared as described (Westerhof et al., 2019). Single cell suspensions of *ex vivo* organs were co-cultured with bmDCs in complete RMPI at a ratio of approximately 10 T cells to 1 DC in the presence of Golgi Plug (BD Bioscience). Co-cultures were incubated at 37°C, 5% CO_2 for 6 hours.

Flow cytometry staining

Single cell suspension were stained with PE or APC-labelled $IA^b/NP_{311-325}$ or APC labelled $D^b/NP_{368-374}$ tetramers (NIH tetramer core) at 37°C, 5% CO_2 for 2 hours in complete RPMI (RPMI with 10% foetal calf serum, 100μg/ml penicillin-streptomycin and 2mM L-glutamine) containing Fc block (24G2). Anti-CX3CR1 BV711 (BioLegend SA011F11) was added with the MHC tetramers. Surface antibodies were added and the cells incubated for a further 20minutes at

4°C. Antibodies used were: anti-CD4 APC-Alexa647(ThermoFisher; clone: RM4-5), anti-CD8 BUV805 (BD 53-6.7) (anti-CD44 BUV395 (BD: IM7), anti-PD-1 PeCy7 (BioLegend: 29F.1A12), anti-PD1 BV605 (BioLegend 29F.1A12), anti-ICOS PerCP-Cy5.5 (ThermoFisher 7E.17G9), anti-CD127 APC (ThermoFisher A7R34), CD103 Pey7 (BioLegend 2E7), anti-CD69 PerCP-Cy5.5 (ThermoFisher H1.2F3) and 'dump' antibodies: B220 (RA3-6B2), F4/80 (BM8) and MHC II (M5114) all on eFluor-450 (ThermoFisher). Cells were stained with a fixable viability dye eFluor 506 (ThermoFisher).

For normalisation of CD127 and Bcl2 expression, the MFI of the EYFP+ cells was divided by the MFI of the naïve (CD44lo) CD4 T cells in the same animal in the same organ.

For intracellular staining, cells were fixed with cytofix/cytoperm (BD Bioscience) for 20 minutes at 4°C and stained in permwash buffer with anti-cytokine antibodies for one hour at room temperature (anti-IFN-γ PE or Brilliant violet 785 (clone: XMG1.2;), anti-TNF Alexa-Fluor-488 or Brilliant Violet 605 (clone: MP6-XT22) anti-IL-2 APC or Brilliant violet 711 (JES6-5H4) from ThermoFisher or BioLegend, anti-Bcl2 PeCy7 (Biolegend; Blc/10C4), anti-Ki67 BV605 (Biolegend; 16A8) and cells washed with permwash buffer. To detect Myc, cells were first stained with unlabelled anti-Myc, cells washed with permwash and then stained with PE-anti-rabbit (both from Cell-Signalling). Stained cells were acquired on a BD LSR or Fortessa and analysed using FlowJo (version 10, Treestar).

BD Rhapsody single cell RNA-seq

CD4 T cells from spleens and lungs of IAV infected TRACE were isolated by CD4 negative selection (Stem Cell) following the manufacturer's instructions. The cells were activated with IAV-Ag-DCs for 4 hours and then stained with anti-CD4 APC-Alexa647, anti-CD44-PerCP-Cy5.5, anti-MHCII-e450, anti-B220-e450, CD8-e450, F4/80-e450, and CD45 Sample Tags (BD Bioscience, see Supplementary Excel file 1) to enable multiplexing and AbSeq antibodies to ICOS (AMM2072) and PD1 (AMM2138). $CD44^{hi}$/EYFP+ and $CD44^{lo}$/EYFP negative cells from combined spleen or lung samples were FACS sorted on an ARIA IIU and cells transferred into BD Rhapsody Sample Buffer and loaded onto a scRNA-seq Rhapsody Cartridge (5000 EYFPnegative $CD44^{lo}$ spleen cells; 5000 EYFP+$CD44^{hi}$ spleen cells; and 1000 EYFP+$CD44^{hi}$ lung cells. Manufacturer's instructions (Mouse VDJ CDR3 library preparation) were followed to prepare libraries for sequencing with the BD Rhapsody Immune response targeted panel (mouse), additional custom made primers (Supplementary excel file 1), sample Tags and VDJ CDR3. Pair-end sequencing was performed by Novogene on an Illumina MiSeq PE250.

Single cell RNA-seq analysis

Data were initially processed on SevenBridges and then analysed predominantly using Seurat (V4.2.0)(Hao et al., 2021) and scRepertoire(V1.7.2)(Borcherding et al., 2020). All analysis code is available at https://github.com/JonathanNoonan/Westerhof_2023. Briefly, to perform dimensionality reduction: count data was normalised using scTransform prior to principal component analysis, Uniform Manifold Approximation and Projection (UMAP) dimensional reduction, Nearest-Neighbour graph construction and cluster determination within the Seurat package, and dimensionality reduction performed. Log normalising and scaling of the count data was conducted prior to differential gene expression analysis. To test for differential gene expression, the FindAllMarkers function was used (min.pct = 0.4 & minLogFC = 0.25, model.use = MAST). Only genes with a Bonferroni corrected p value <0.05 were considered statistically different. For TCR analysis, clonal expansion was calculated based on the same TCR being detected once (Single Clone) or multiple times within the same animal. All TCR analysis utilised stock or customised code from the scRepertoire package. Further packages used for data analysis, organisation and visualisation included: workflowR (Blischak et al., 2019), dplyr, ggplot2, cowplot, ggVenn, circlize, plot1cell (Wu et al., 2022) and ComplexHeatmap.

Statistical analysis

All data other than scRNAseq were analysed using Prism version 9 software (GraphPad). Differences between groups were analysed by unpaired ANOVAs or T-tests as indicated in figure legends. Multi-group non-parametric data were analysed using Kruskal-Wallis testing with a *post hoc* Dunn's test. P-value correction for multiple comparison was performed using the Benjamini-Hochberg method. In all figures * represents a p value of <0.05; **: p<0.01, ***: p<0.001, ****: p<0.0001

Data availability

scRNA-seq data deposited on GEO, accession number: GSE220588.

Supplemental material

Included in the supplemental material are:

Supplementary Figure 1: Example gating of IAV specific CD4 and CD8 T cells identified by MHC tetramers

Supplementary Figure 2: Primary responding cytokine+ CD4 T cells are more sensitive to a decrease in peptide dose than memory CD4 T cells or CD8 T cells

Supplementary Figure 3: TRACE mice enable identification of CD4 T cells responding to IAV infection

Supplementary Figure 4: scRNAseq reveals heterogeneity in the memory CD4 T cell pool

Supplementary Figure 5: Previous infection with IAV leads to a protective response following re-challenge infection but a limited increase in cytokine+ T cells

Supplementary Table 1: Differentially expressed genes from the scRNAseq analysis

Supplementary File 1: Sample Tag sequences, TCR primers and additional genes for the scRNAseq analysis

CRediT authorship contribution statement

LMW: conception, investigation, formal analysis, visualization, writing - original draft and reviewing/editing. JN: formal analysis, data curation, software, visualization, writing - reviewing and editing. KEH: investigation, formal analysis, writing - reviewing and editing. ETC: investigation, formal analysis, writing - reviewing and editing, ZC: investigation, formal analysis, writing -reviewing and editing, TP: investigation, writing - reviewing and editing. MRJ: formal analysis, writing – reviewing and editing. NB: software, writing – reviewing and editing. MKLM: Supervision, project management, funding acquisition, conception, investigation, formal analysis, visualization, writing -original draft and reviewing.

Acknowledgments

We thank the staff within the School of Infection and Immunity Flow Cytometry Facility and Biological Services at the University of Glasgow for technical assistance. Thank you to members of the Kurowska-Stolarska for technical assistance with the BD Rhapsody experiment. Thank you to Prof James Brewer and Dr Edward Roberts for critical review of the manuscript and the MacLeod lab for discussions. We thank the NIH tetramer core facility for the provision of IA^b-$NP_{311-325}$ and D^b/NP NP_{368-74} tetramers. The work was funded by a GLAZgo Discovery Centre PhD fellowship to LMW, a Marie Curie Fellowship (334430) and a Wellcome Trust Investigator Award (210703/Z/18/Z) to MKLM.

The authors have no competing interests to declare.

Figures legends

Figure 1

Memory IAV specific CD4 and CD8 T cells can be tracked using MHC tetramers and via ex vivo *cytokine responses*

C57BL/6 mice were infected i.n. with IAV on day 0 and injected i.v. with fluorescently labelled anti-CD45 3 minutes prior to removal of organs for analysis. Single cell suspensions of spleens, mediastinal draining lymph node (dLN), and lung were examined after 9, 30 or 70 days. Single cell suspensions were either stained with $IA^b/NP_{311-325}$ or $D^b/NP_{368-374}$ tetramers or cells were restimulated in the presence of Golgi Plug for 6hours with $NP_{311-325}$ and $NP_{368-374}$ peptides loaded onto bmDCs (A). Example Flow cytometry plots of the IAV specific cells in the spleen, cells gated as shown in Supplementary Figure 1A (B). The percentages of IAV specific cells that bound to the i.v. injected anti-CD45 was analysed at each time point, cells gated as in Supplementary Figure 1B (C). The phenotype of MHC tetramer+ CD4 and CD8 T cells at each time point was examined in each organ (D). Data are from two independent time course experiments with a total of 7-8 mice/time point. In C-D, symbols show the mean of the group and error bars are SEM. Statistical difference tested by ANOVA followed by a Dunnett's multiple comparison test for analyses between time points and by a Tukey's test between organs, *: p<0.05, **:p<0.01, ***:p<0.001, ****:p<0.0001.

Figure 2

Influenza virus specific IFNγ+ *CD4 and CD8 T cells contract more slowly that IAV specific cells detected by MHC tetramers*

C57BL/6 mice were infected i.n. with IAV on day 0 and injected i.v. with fluorescently labelled anti-CD45 (CD45iv) 3 minutes prior to removal of organs for analysis. Single cell suspensions of spleens, mediastinal draining lymph node (dLN), and lung were examined after 9, 30 or 70 days and either stained with MHCII/NP or MHCI/ NP tetramers, or activated with $NP_{311-325}$ and $NP_{368-374}$ peptide loaded bmDCs to determine the numbers of MHC tetramer or IFNγ+ CD4 (A) or CD8 T cells (B). The numbers of IL-2+ and TNF+ T cells were also examined (C-D) Data are from two independent time course experiments with a total of 7-8 mice/time point. Y-axis set at the limit of detection and errors are SEM. Significance tested by a Kruskal-Wallis test followed by a Dunn's multiple comparison test with Benjamini-Hochberg correction for multiple comparisons *: p<0.05, **:p<0.01, ***:p<0.001, ****:p<0.0001.

Figure 3

Cytokine producing T cells express higher levels of CD127 and Bcl2 than non-cytokine+ T cells

TRACE mice were infected i.n. with IAV on day 0 and injected i.v. with fluorescently labelled anti-CD45 3 minutes prior to removal of organs for analysis at day 40. Single cell suspensions of spleens, mediastinal draining lymph node (dLN), and lung were examined following incubation with IAV-Ag+ bmDCs. CD45iv negative IAV specific CD4 T cells were detected by flow cytometry. Example FACS plots from the spleen are gated on live CD4+ dump negative, CD45i.v. negative cells and as indicated (cytokine negative: grey; IFNγ, IL-2 and/or TNF+: red) (A). Data are from three independent experiments with a total of 5-8 mice/time point and normalised by dividing the MFI on EYFP+ cells by the MFI of naïve $CD44^{lo}$ CD4 T cells from the same mouse and organ. In B, symbols represent a mouse and the lines shows the means, error bars are SEM. Samples from some dLNs and lungs were excluded as the numbers of EYFP+ cells collected were too low for analysis. Significance tested via a Friedman paired analysis with Dunn's multiple comparison test, *: p<0.05, **:p<0.01.

Figure 4

Triple cytokine+ cells are less likely to decline than single IFNγ+ T cells

C57BL/6 mice were infected i.n. with IAV on day 0 and injected i.v. with fluorescently labelled anti-CD45 3 minutes prior to removal of organs for analysis. Single cell suspensions of spleens, mediastinal draining lymph node (dLN), and lung were activated after 9 or 30 days by bmDCs incubated with IAV-Ag preparation. CD45iv negative IAV specific cytokine+ CD4 and CD8 T cells were detected by flow cytometry. Data are from two independent time course experiments with a total of 7-8 mice/time point. Y-axis set at the limit of detection. Samples from some dLNs and lungs were excluded as the numbers of total cells collected were too low for analysis. Symbols represent each mouse, the bar shows the mean of the group and errors are SEM. Significance tested by a Kruskal-Wallis test followed by a Dunn's multiple comparison test with Benjamini-Hockberg correction for multiple comparisons *: $p<0.05$, **:$p<0.01$, ***:$p<0.001$, ****:$p<0.0001$.

Figure 5

Triple cytokine+ CD4 T cells produce more cytokine on a per cell basis than single cytokine+ T cells

C57BL/6 mice were infected i.n. with IAV on day 9 or day 30 and injected i.v. with fluorescently labelled anti-CD45 3 minutes prior to removal of organs for analysis. Single cell suspensions of spleens, mediastinal draining lymph node (dLN), and lung were activated by bmDCs incubated with IAV-Ag. CD45iv negative IAV specific CD4 T cells cytokine+ at day 9 (A) or day 30 (B) T cells were detected by flow cytometry. Each symbol represents a mouse and the line shows the mean of the group with SEM shown. Significant differences were assessed by Friedman's multiple comparison test followed by multiple comparisons with Dunn's multiple comparison test; *: $p<0.05$, **:$p<0.01$, ***:$p<0.001$.

Figure 6

Single IFNγ+ CD4 and CD8 T cells are more likely to be in cell cycle 9 and 30 days after IAV infection than T cells producing multiple cytokines

C57BL/6 mice were infected i.n. with IAV on day 0 and injected i.v. with fluorescently labelled anti-CD45 3 minutes prior to removal of organs for analysis at the indicated time point. Single cell suspensions of spleens, mediastinal draining lymph node (dLN), and lung were activated by bmDCs incubated with IAV-Ag preparation. CD45iv negative cytokine+ T cells were detected by flow cytometry to detect Ki67 (A-D) or PD1 and ICOS (E,F) expression by cytokine producing T cells (CD4: A, C, E, F; CD8: B, D). Data are from two independent time course experiments with a total of 7-8 mice/time point or two separate experiments in E-F. In C-F, each symbol represents a mouse and the horizontal line shows the mean of the group. In C-F, significance tested via paired Friedman analysis with Dunn's multiple comparison test *: $p<0.05$, ***:$p<0.001$.

Figure 7

Triple cytokine+ CD4 T cells in the spleen express high levels of CD127 and Bcl2

TRACE mice were infected i.n. with IAV on day 0 and injected i.v. with fluorescently labelled anti-CD45 3 minutes prior to removal of organs for analysis on day 40. Single cell suspensions of spleens, mediastinal draining lymph node (dLN), and lung were activated by bmDCs incubated with IAV-Ag preparation. CD45iv negative IAV specific cytokine+ CD4 T cells were detected by flow cytometry and normalised by dividing the MFI on EYFP+ cells by the MFI of naïve $CD44^{lo}$ CD4 T cells from the same mouse and organ. Data are combined from 2-3 experiments with 4-5 mice per experiment, each symbol represents a mouse and the line shows the mean of the group, error bars are SEM. Significance tested via ANOVA with a Dunn's multiple comparison test, *: $p<0.05$, ***:$p<0.001$, ****:$p<0.00001$.

Figure 8

Triple cytokine+ CD4 T cells have a pro-survival transcriptomal signature

TRACE mice were infected with IAV and 40 days later injected with anti-CD45 3minutes prior to removal of spleens and lungs. Isolated CD4 T cells were activated for 4 hours with IAV-Ag DCs and the CD45iv negative CD4+CD44^{hi}EYFP+ cells (spleens and lung) and CD4+CD44^{lo}EYFPnegative (spleens) cells were FACS sorted and their transcriptomes examined by scRNAseq. UMAP of one naïve/central memory cluster, one Treg cluster, and 10 memory clusters. The radial tracks around the UMAP reflect the numerical representation of each cluster, and the mouse/tissue origin within each cluster, on a logarithmic axis (A). DEGs in single, double, and triple cytokine+ clusters identified by comparison between the indicated populations and all other clusters (B). The normalised MFI of Myc by single, double, and triple cytokine+ cells in CD4 and CD8 T cells from C57BL/6 IAV infected mice examined at day 40 post infection; expression was normalised by dividing each sample's MFI by the MFI on naïve CD4+ cells in same sample (C). Expression of mRNA for chemokine receptors and with cell survival molecules from the scRNAseq analysis (D,E). Data in A, B, D, and E are from one experiment with cells from 4 mice. In C, data are from 2 independent experiments with each symbol representing one mouse and the horizontal line showing the mean of the groups; significance tested by paired ANOVA with Tukey's multiple comparison test, *: $p<0.05$.

Figure 9

Identified TCR clones are found in all memory clusters

scRNAseq analysis described in Figure 8 was integrated with single cell TCR CDR3 analysis. Large, medium and single clones identified by TCR CDR3 sequencing are displayed for each cluster and proportion of T cells with indicated clonal expansions shown (A). Enriched clones are overlaid on the scRNAseq UMAP for each animal and coloured by the magnitude of expansion (B). To highlight the extent to which clones were shared across clusters, clones found within each memory cluster were identified and displayed on the UMAP (C). To provide higher resolution these data are presented as a chord diagram, highlighting the inter-cluster relationship of individual clones (D). The limited overlap of identified clones between mice is displayed as a Venn diagram (E).

Figure 10

Triple cytokine+ T cells are less likely to be in cell cycle than single IFNγ+ T cells following challenge infection

C57BL/6 mice were infected i.n. with IAV on day 0. On day 30, some of these animals were infected with X31 IAV i.n. and 5 (A-F) or 35 days (G-H) later all mice were injected i.v. with fluorescently labelled anti-CD45 3 minutes prior to removal of organs for analysis. Single cell suspensions of spleens, mediastinal draining lymph node (dLN), and lung were activated for 6 hours in the presence of Golgi Plug by bmDCs incubated with IAV-Ag preparation. CD45iv negative IAV specific IFNγ+ CD4 T cells (A,C,E,G) or CD8 T cells (B,D,F,H) were detected by flow to detect either IFNγ+ cells or IFNγ+ T cells that were Ki67+. Data are from two independent experiments with a total of 7-8 mice. Symbols represent each mouse and the horizontal line shows the mean of the group (A-F), in G-H error bars are SEM. In A-D significance tested by Mann-Whitney. In E-F, significance tested via ANOVA and Dunn's. In all graphs: *: $p<0.05$, **:$p<0.01$, ***:$p<0.001$, ****:$p<0.0001$.

References

Alam, F., A. Singh, V. Flores-Malavet, S. Sell, A.M. Cooper, S.L. Swain, K.K. McKinstry, and T.M. Strutt. 2020. CD25-Targeted IL-2 Signals Promote Improved Outcomes of Influenza Infection and Boost Memory CD4 T Cell Formation. *J Immunol* 204:3307-3314.

Almeida, J.R., D.A. Price, L. Papagno, Z.A. Arkoub, D. Sauce, E. Bornstein, T.E. Asher, A. Samri, A. Schnuriger, I. Theodorou, D. Costagliola, C. Rouzioux, H. Agut, A.G. Marcelin, D. Douek, B. Autran, and V. Appay. 2007. Superior control of HIV-1 replication by CD8+ T cells is reflected by their avidity, polyfunctionality, and clonal turnover. *J Exp Med* 204:2473-2485.

Blischak, J.D., P. Carbonetto, and M. Stephens. 2019. Creating and sharing reproducible research code the workflowr way. *F1000Res* 8:1749.

Bonsignori, M., H.X. Liao, F. Gao, W.B. Williams, S.M. Alam, D.C. Montefiori, and B.F. Haynes. 2017. Antibody-virus co-evolution in HIV infection: paths for HIV vaccine development. *Immunol Rev* 275:145-160.

Borcherding, N., N.L. Bormann, and G. Kraus. 2020. scRepertoire: An R-based toolkit for single-cell immune receptor analysis. *F1000Res* 9:47.

Bot, A., S. Bot, and C.A. Bona. 1998. Protective role of gamma interferon during the recall response to influenza virus. *J Virol* 72:6637-6645.

Bresser, K., L. Kok, A.C. Swain, L.A. King, L. Jacobs, T.S. Weber, L. Perie, K.R. Duffy, R.J. de Boer, F.A. Scheeren, and T.N. Schumacher. 2022. Replicative history marks transcriptional and functional disparity in the CD8(+) T cell memory pool. *Nat Immunol* 23:791-801.

Buccitelli, C., and M. Selbach. 2020. mRNAs, proteins and the emerging principles of gene expression control. *Nat Rev Genet* 21:630-644.

Casey, K.A., K.A. Fraser, J.M. Schenkel, A. Moran, M.C. Abt, L.K. Beura, P.J. Lucas, D. Artis, E.J. Wherry, K. Hogquist, V. Vezys, and D. Masopust. 2012. Antigen-independent differentiation and maintenance of effector-like resident memory T cells in tissues. *J Immunol* 188:4866-4875.

Catron, D.M., L.K. Rusch, J. Hataye, A.A. Itano, and M.K. Jenkins. 2006. CD4+ T cells that enter the draining lymph nodes after antigen injection participate in the primary response and become central-memory cells. *J Exp Med* 203:1045-1054.

Croft, M., T. So, W. Duan, and P. Soroosh. 2009. The significance of OX40 and OX40L to T-cell biology and immune disease. *Immunol Rev* 229:173-191.

Crotty, S. 2019. T Follicular Helper Cell Biology: A Decade of Discovery and Diseases. *Immunity* 50:1132-1148.

Darrah, P.A., D.T. Patel, P.M. De Luca, R.W. Lindsay, D.F. Davey, B.J. Flynn, S.T. Hoff, P. Andersen, S.G. Reed, S.L. Morris, M. Roederer, and R.A. Seder. 2007. Multifunctional TH1 cells define a correlate of vaccine-mediated protection against Leishmania major. *Nat Med* 13:843-850.

DeBerge, M.P., K.H. Ely, and R.I. Enelow. 2014. Soluble, but not transmembrane, TNF-alpha is required during influenza infection to limit the magnitude of immune responses and the extent of immunopathology. *J Immunol* 192:5839-5851.

Ely, K.H., T. Cookenham, A.D. Roberts, and D.L. Woodland. 2006. Memory T cell populations in the lung airways are maintained by continual recruitment. *J Immunol* 176:537-543.

Epstein, S.L., C.Y. Lo, J.A. Misplon, and J.R. Bennink. 1998. Mechanism of protective immunity against influenza virus infection in mice without antibodies. *J Immunol* 160:322-327.

Flores-Fernandez, R., A. Aponte-Lopez, M.C. Suarez-Arriaga, P. Gorocica-Rosete, A. Pizana-Venegas, L. Chavez-Sanchez, F. Blanco-Favela, E.M. Fuentes-Panana, and A.K. Chavez-Rueda. 2021. Prolactin Rescues Immature B Cells from Apoptosis-Induced BCR-Aggregation through STAT3, Bcl2a1a, Bcl2l2, and Birc5 in Lupus-Prone MRL/lpr Mice. *Cells* 10:

Genesca, M., T. Rourke, J. Li, K. Bost, B. Chohan, M.B. McChesney, and C.J. Miller. 2007. Live attenuated lentivirus infection elicits polyfunctional simian immunodeficiency virus Gag-specific CD8+ T cells with reduced apoptotic susceptibility in rhesus macaques that control virus replication after challenge with pathogenic SIVmac239. *J Immunol* 179:4732-4740.

Gerlach, C., E.A. Moseman, S.M. Loughhead, D. Alvarez, A.J. Zwijnenburg, L. Waanders, R. Garg, J.C. de la Torre, and U.H. von Andrian. 2016. The Chemokine Receptor CX3CR1 Defines Three Antigen-Experienced CD8 T Cell Subsets with Distinct Roles in Immune Surveillance and Homeostasis. *Immunity* 45:1270-1284.

Gray, J.I., S. Al-Khabouri, F. Morton, E.T. Clambey, L. Gapin, J.L. Matsuda, J.W. Kappler, P. Marrack, P. Garside, T.D. Otto, and M.K.L. MacLeod. 2021. Tolerance induction in memory CD4 T cells is partial and reversible. *Immunology* 162:68-83.

Hao, Y., S. Hao, E. Andersen-Nissen, W.M. Mauck, 3rd, S. Zheng, A. Butler, M.J. Lee, A.J. Wilk, C. Darby, M. Zager, P. Hoffman, M. Stoeckius, E. Papalexi, E.P. Mimitou, J. Jain, A. Srivastava, T. Stuart, L.M. Fleming, B. Yeung, A.J. Rogers, J.M. McElrath, C.A. Blish, R. Gottardo, P. Smibert, and R. Satija. 2021. Integrated analysis of multimodal single-cell data. *Cell* 184:3573-3587 e3529.

Hayward, A.C., L. Wang, N. Goonetilleke, E.B. Fragaszy, A. Bermingham, A. Copas, O. Dukes, E.R. Millett, I. Nazareth, J.S. Nguyen-Van-Tam, J.M. Watson, M. Zambon, G. Flu Watch, A.M. Johnson, and A.J. McMichael. 2015. Natural T Cell-mediated Protection against Seasonal and Pandemic Influenza. Results of the Flu Watch Cohort Study. *Am J Respir Crit Care Med* 191:1422-1431.

Heiny, A.T., O. Miotto, K.N. Srinivasan, A.M. Khan, G.L. Zhang, V. Brusic, T.W. Tan, and J.T. August. 2007. Evolutionarily conserved protein sequences of influenza a viruses, avian and human, as vaccine targets. *PLoS One* 2:e1190.

Homann, D., L. Teyton, and M.B. Oldstone. 2001. Differential regulation of antiviral T-cell immunity results in stable CD8+ but declining CD4+ T-cell memory. *Nat Med* 7:913-919.

Inaba, K., M. Inaba, N. Romani, H. Aya, M. Deguchi, S. Ikehara, S. Muramatsu, and R.M. Steinman. 1992. Generation of large numbers of dendritic cells from mouse bone marrow cultures supplemented with granulocyte/macrophage colony-stimulating factor. *J Exp Med* 176:1693-1702.

Jelley-Gibbs, D.M., D.M. Brown, J.P. Dibble, L. Haynes, S.M. Eaton, and S.L. Swain. 2005. Unexpected prolonged presentation of influenza antigens promotes CD4 T cell memory generation. *J Exp Med* 202:697-706.

Krishnamoorthy, V., S. Kannanganat, M. Maienschein-Cline, S.L. Cook, J. Chen, N. Bahroos, E. Sievert, E. Corse, A. Chong, and R. Sciammas. 2017. The IRF4 Gene Regulatory Module Functions as a Read-Write Integrator to Dynamically Coordinate T Helper Cell Fate. *Immunity* 47:481-497 e487.

Kumar, B.V., W. Ma, M. Miron, T. Granot, R.S. Guyer, D.J. Carpenter, T. Senda, X. Sun, S.H. Ho, H. Lerner, A.L. Friedman, Y. Shen, and D.L. Farber. 2017. Human Tissue-Resident Memory T Cells Are Defined by Core Transcriptional and Functional Signatures in Lymphoid and Mucosal Sites. *Cell Rep* 20:2921-2934.

Kunzli, M., D. Schreiner, T.C. Pereboom, N. Swarnalekha, L.C. Litzler, J. Lotscher, Y.I. Ertuna, J. Roux, F. Geier, R.P. Jakob, T. Maier, C. Hess, J.J. Taylor, and C.G. King. 2020. Long-lived T follicular helper cells retain plasticity and help sustain humoral immunity. *Sci Immunol* 5:

Kwissa, M., R.R. Amara, H.L. Robinson, B. Moss, S. Alkan, A. Jabbar, F. Villinger, and B. Pulendran. 2007. Adjuvanting a DNA vaccine with a TLR9 ligand plus Flt3 ligand results in enhanced cellular immunity against the simian immunodeficiency virus. *J Exp Med* 204:2733-2746.

Leonard, W.J., J.X. Lin, and J.J. O'Shea. 2019. The gammac Family of Cytokines: Basic Biology to Therapeutic Ramifications. *Immunity* 50:832-850.

Liang, S., K. Mozdzanowska, G. Palladino, and W. Gerhard. 1994. Heterosubtypic immunity to influenza type A virus in mice. Effector mechanisms and their longevity. *J Immunol* 152:1653-1661.

Lindenstrom, T., E.M. Agger, K.S. Korsholm, P.A. Darrah, C. Aagaard, R.A. Seder, I. Rosenkrands, and P. Andersen. 2009. Tuberculosis subunit vaccination provides long-term protective immunity characterized by multifunctional CD4 memory T cells. *J Immunol* 182:8047-8055.

MacLean, A.J., N. Richmond, L. Koneva, M. Attar, C.A.P. Medina, E.E. Thornton, A.C. Gomes, A. El-Turabi, M.F. Bachmann, P. Rijal, T.K. Tan, A. Townsend, S.N. Sansom, O. Bannard, and T.I. Arnon. 2022. Secondary influenza challenge triggers resident memory B cell migration and rapid relocation to boost antibody secretion at infected sites. *Immunity* 55:718-733 e718.

Marchingo, J.M., L.V. Sinclair, A.J. Howden, and D.A. Cantrell. 2020. Quantitative analysis of how Myc controls T cell proteomes and metabolic pathways during T cell activation. *Elife* 9:

Masopust, D., and A.G. Soerens. 2019. Tissue-Resident T Cells and Other Resident Leukocytes. *Annu Rev Immunol* 37:521-546.

McKinstry, K.K., T.M. Strutt, Y. Kuang, D.M. Brown, S. Sell, R.W. Dutton, and S.L. Swain. 2012. Memory CD4+ T cells protect against influenza through multiple synergizing mechanisms. *J Clin Invest* 122:2847-2856.

Metais, J.Y., T. Winkler, J.T. Geyer, R.T. Calado, P.D. Aplan, M.A. Eckhaus, and C.E. Dunbar. 2012. BCL2A1a over-expression in murine hematopoietic stem and progenitor cells decreases apoptosis and results in hematopoietic transformation. *PLoS One* 7:e48267.

Mueller, S.N., T. Gebhardt, F.R. Carbone, and W.R. Heath. 2013. Memory T cell subsets, migration patterns, and tissue residence. *Annu Rev Immunol* 31:137-161.

Nguyen, Q.P., T.Z. Deng, D.A. Witherden, and A.W. Goldrath. 2019. Origins of CD4(+) circulating and tissue-resident memory T-cells. *Immunology* 157:3-12.

Nishimura, H., T. Yajima, H. Muta, E.R. Podack, K. Tani, and Y. Yoshikai. 2005. A novel role of CD30/CD30 ligand signaling in the generation of long-lived memory CD8+ T cells. *J Immunol* 175:4627-4634.

Pizzolla, A., T.H.O. Nguyen, J.M. Smith, A.G. Brooks, K. Kedzieska, W.R. Heath, P.C. Reading, and L.M. Wakim. 2017. Resident memory CD8(+) T cells in the upper respiratory tract prevent pulmonary influenza virus infection. *Sci Immunol* 2:

Pramanik, J., X. Chen, G. Kar, J. Henriksson, T. Gomes, J.E. Park, K. Natarajan, K.B. Meyer, Z. Miao, A.N.J. McKenzie, B. Mahata, and S.A. Teichmann. 2018. Genome-wide analyses reveal the IRE1a-XBP1 pathway promotes T helper cell differentiation by resolving secretory stress and accelerating proliferation. *Genome Med* 10:76.

Sasson, S.C., C.L. Gordon, S.N. Christo, P. Klenerman, and L.K. Mackay. 2020. Local heroes or villains: tissue-resident memory T cells in human health and disease. *Cell Mol Immunol* 17:113-122.

Slutter, B., N. Van Braeckel-Budimir, G. Abboud, S.M. Varga, S. Salek-Ardakani, and J.T. Harty. 2017. Dynamics of influenza-induced lung-resident memory T cells underlie waning heterosubtypic immunity. *Sci Immunol* 2:

Son, Y.M., I.S. Cheon, Y. Wu, C. Li, Z. Wang, X. Gao, Y. Chen, Y. Takahashi, Y.X. Fu, A.L. Dent, M.H. Kaplan, J.J. Taylor, W. Cui, and J. Sun. 2021. Tissue-resident CD4(+) T helper cells assist the development of protective respiratory B and CD8(+) T cell memory responses. *Sci Immunol* 6:

Soudja, S.M., C. Chandrabos, E. Yakob, M. Veenstra, D. Palliser, and G. Lauvau. 2014. Memory-T-cell-derived interferon-gamma instructs potent innate cell activation for protective immunity. *Immunity* 40:974-988.

Sridhar, S., S. Begom, A. Bermingham, K. Hoschler, W. Adamson, W. Carman, T. Bean, W. Barclay, J.J. Deeks, and A. Lalvani. 2013. Cellular immune correlates of protection against symptomatic pandemic influenza. *Nat Med* 19:1305-1312.

Stoiber, D., S. Stockinger, P. Steinlein, J. Kovarik, and T. Decker. 2001. Listeria monocytogenes modulates macrophage cytokine responses through STAT serine phosphorylation and the induction of suppressor of cytokine signaling 3. *J Immunol* 166:466-472.

Stone, E.L., M. Pepper, C.D. Katayama, Y.M. Kerdiles, C.Y. Lai, E. Emslie, Y.C. Lin, E. Yang, A.W. Goldrath, M.O. Li, D.A. Cantrell, and S.M. Hedrick. 2015. ICOS coreceptor signaling inactivates the transcription factor FOXO1 to promote Tfh cell differentiation. *Immunity* 42:239-251.

Strutt, T.M., K.K. McKinstry, J.P. Dibble, C. Winchell, Y. Kuang, J.D. Curtis, G. Huston, R.W. Dutton, and S.L. Swain. 2010. Memory CD4+ T cells induce innate responses independently of pathogen. *Nat Med* 16:558-564, 551p following 564.

Swarnalekha, N., D. Schreiner, L.C. Litzler, S. Iftikhar, D. Kirchmeier, M. Kunzli, Y.M. Son, J. Sun, E.A. Moreira, and C.G. King. 2021. T resident helper cells promote humoral responses in the lung. *Sci Immunol* 6:

Takamura, S., S. Kato, C. Motozono, T. Shimaoka, S. Ueha, K. Matsuo, K. Miyauchi, T. Masumoto, A. Katsushima, T. Nakayama, M. Tomura, K. Matsushima, M. Kubo, and M. Miyazawa. 2019. Interstitial-resident memory CD8(+) T cells sustain frontline epithelial memory in the lung. *J Exp Med* 216:2736-2747.

Tang, C., H. Yamada, K. Shibata, H. Muta, W. Wajjwalku, E.R. Podack, and Y. Yoshikai. 2008. A novel role of CD30L/CD30 signaling by T-T cell interaction in Th1 response against mycobacterial infection. *J Immunol* 181:6316-6327.

Tao, K., P.L. Tzou, J. Nouhin, R.K. Gupta, T. de Oliveira, S.L. Kosakovsky Pond, D. Fera, and R.W. Shafer. 2021. The biological and clinical significance of emerging SARS-CoV-2 variants. *Nat Rev Genet* 22:757-773.

Teijaro, J.R., D. Verhoeven, C.A. Page, D. Turner, and D.L. Farber. 2010. Memory CD4 T cells direct protective responses to influenza virus in the lungs through helper-independent mechanisms. *J Virol* 84:9217-9226.

Tsang, T.K., K.T. Lam, Y. Liu, V.J. Fang, X. Mu, N.H.L. Leung, J.S.M. Peiris, G.M. Leung, B.J. Cowling, and W. Tu. 2022. Investigation of CD4 and CD8 T cell-mediated protection against influenza A virus in a cohort study. *BMC Med* 20:230.

Turtle, L., T. Bali, G. Buxton, S. Chib, S. Chan, M. Soni, M. Hussain, H. Isenman, P. Fadnis, M.M. Venkataswamy, V. Satishkumar, P. Lewthwaite, A. Kurioka, S. Krishna, M.V. Shankar, R. Ahmed, A. Begum, V. Ravi, A. Desai, S. Yoksan, S. Fernandez, C.B. Willberg, H.N. Kloverpris, C. Conlon, P. Klenerman, V. Satchidanandam, and T. Solomon. 2016. Human T cell responses to Japanese encephalitis virus in health and disease. *J Exp Med* 213:1331-1352.

Wang, M., K. Lamberth, M. Harndahl, G. Roder, A. Stryhn, M.V. Larsen, M. Nielsen, C. Lundegaard, S.T. Tang, M.H. Dziegiel, J. Rosenkvist, A.E. Pedersen, S. Buus, M.H. Claesson, and O. Lund. 2007. CTL epitopes for influenza A including the H5N1 bird flu; genome-, pathogen-, and HLA-wide screening. *Vaccine* 25:2823-2831.

Wang, R., H. Xie, Z. Huang, W. Shang, and Z. Sun. 2012. Developing and activated T cell survival depends on differential signaling pathways to regulate anti-apoptotic Bcl-x(L). *Clin Dev Immunol* 2012:632837.

Webster, R.G., and E.A. Govorkova. 2014. Continuing challenges in influenza. *Ann N Y Acad Sci* 1323:115-139.

Westerhof, L.M., K. McGuire, L. MacLellan, A. Flynn, J.I. Gray, M. Thomas, C.S. Goodyear, and M.K. MacLeod. 2019. Multifunctional cytokine production reveals functional superiority of memory CD4 T cells. *Eur J Immunol* 49:2019-2029.

Wherry, E.J., V. Teichgraber, T.C. Becker, D. Masopust, S.M. Kaech, R. Antia, U.H. von Andrian, and R. Ahmed. 2003. Lineage relationship and protective immunity of memory CD8 T cell subsets. *Nat Immunol* 4:225-234.

Wilkinson, T.M., C.K. Li, C.S. Chui, A.K. Huang, M. Perkins, J.C. Liebner, R. Lambkin-Williams, A. Gilbert, J. Oxford, B. Nicholas, K.J. Staples, T. Dong, D.C. Douek, A.J. McMichael, and X.N. Xu. 2012. Preexisting influenza-specific CD4+ T cells correlate with disease protection against influenza challenge in humans. *Nat Med* 18:274-280.

Wirth, T.C., H.H. Xue, D. Rai, J.T. Sabel, T. Bair, J.T. Harty, and V.P. Badovinac. 2010. Repetitive antigen stimulation induces stepwise transcriptome diversification but preserves a core signature of memory CD8(+) T cell differentiation. *Immunity* 33:128-140.

Wu, H., R. Gonzalez Villalobos, X. Yao, D. Reilly, T. Chen, M. Rankin, E. Myshkin, M.D. Breyer, and B.D. Humphreys. 2022. Mapping the single-cell transcriptomic response of murine diabetic kidney disease to therapies. *Cell Metab* 34:1064-1078 e1066.

Zammit, D.J., D.L. Turner, K.D. Klonowski, L. Lefrancois, and L.S. Cauley. 2006. Residual antigen presentation after influenza virus infection affects CD8 T cell activation and migration. *Immunity* 24:439-449.

Zheng, M.Z.M., and L.M. Wakim. 2022. Tissue resident memory T cells in the respiratory tract. *Mucosal Immunol* 15:379-388.

Figure 1: Memory IAV specific CD4 and CD8 T cells can be tracked using MHC tetramers and via *ex vivo* cytokine responses

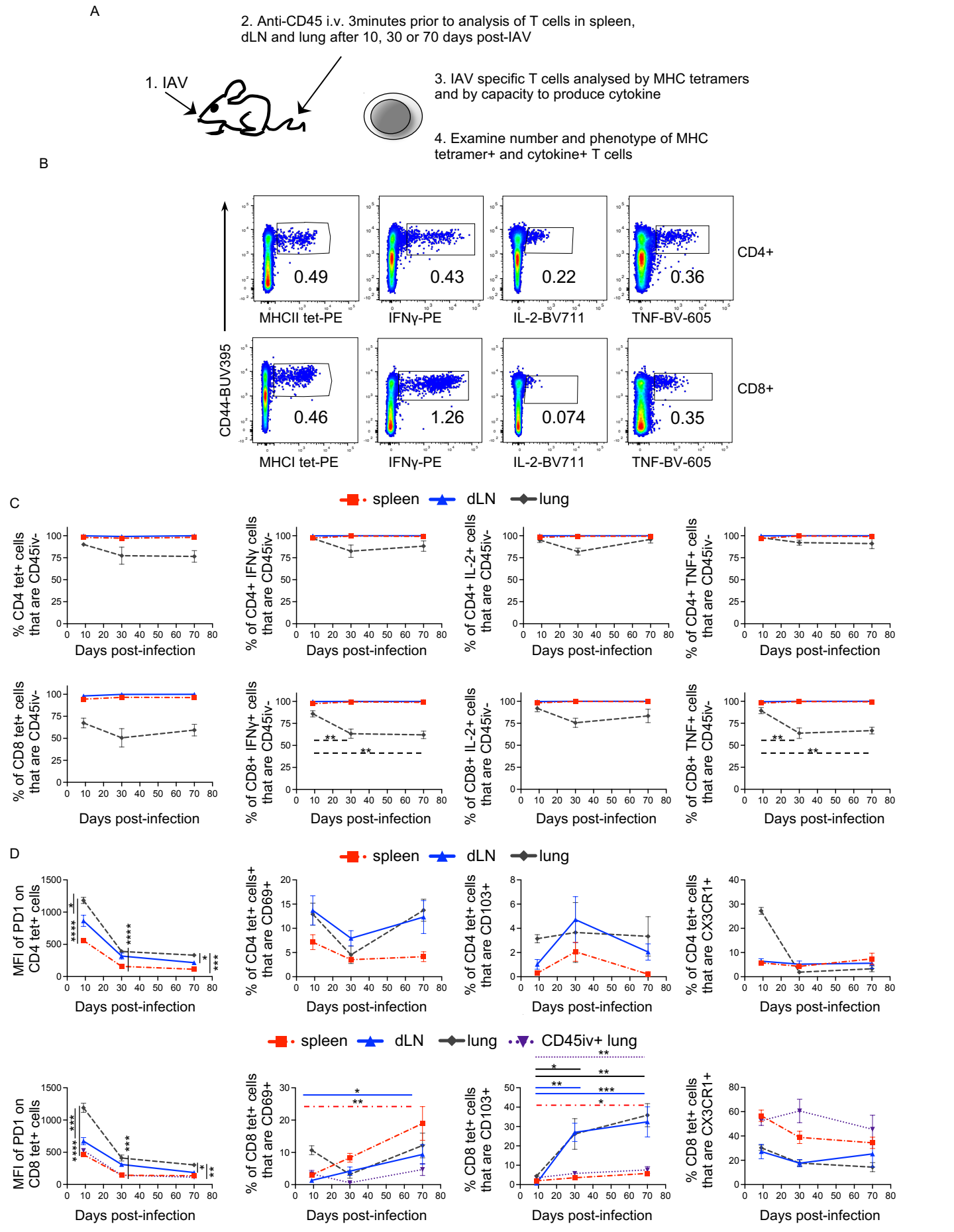

Figure 2 Influenza virus specific IFNγ+ CD4 and CD8 T cells contract more slowly than IAV specific T cells detected by MHC tetramers

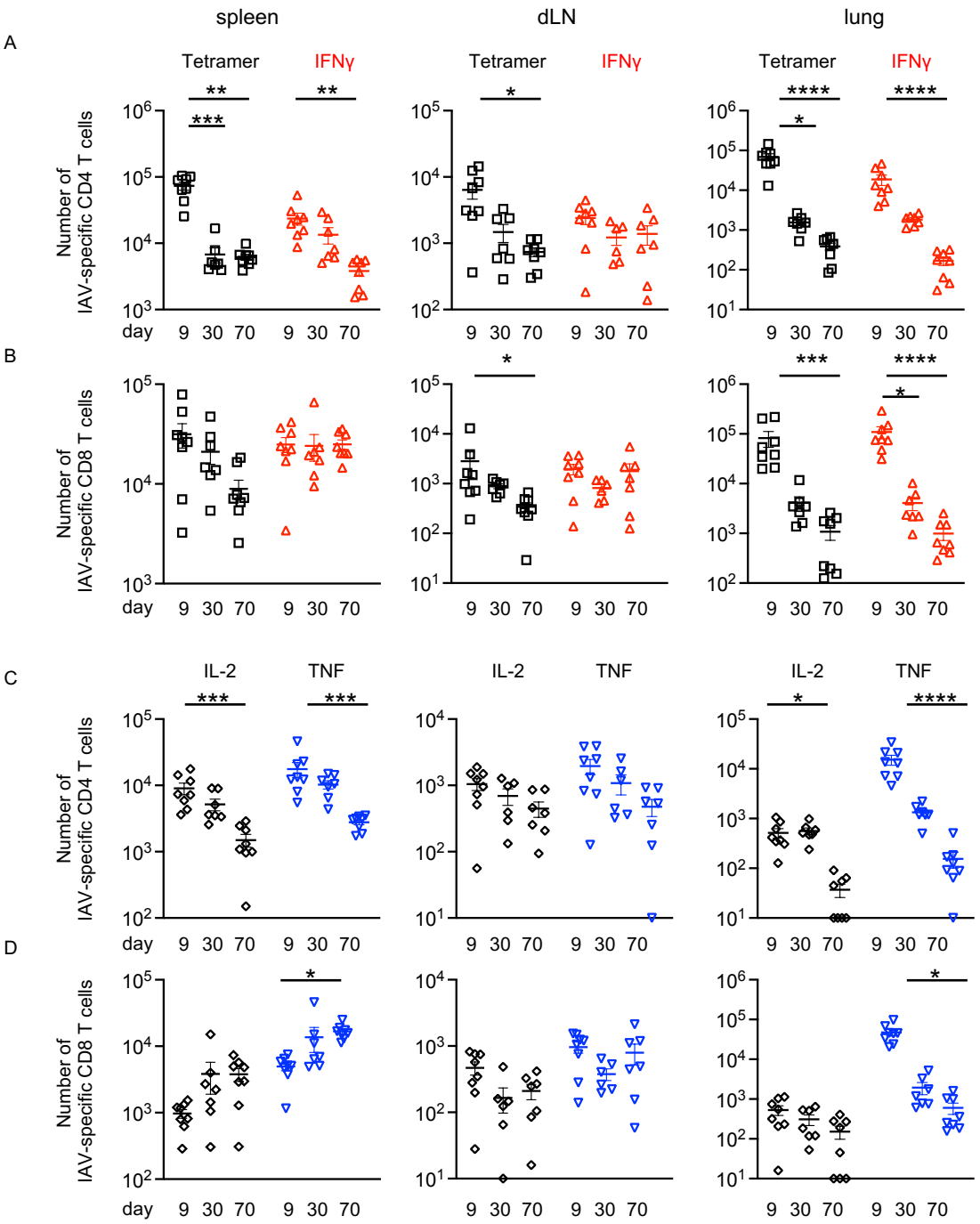

Figure 3: Cytokine+ CD4 T cells express higher levels of CD127 and Bcl2 than non-cytokine+ cells

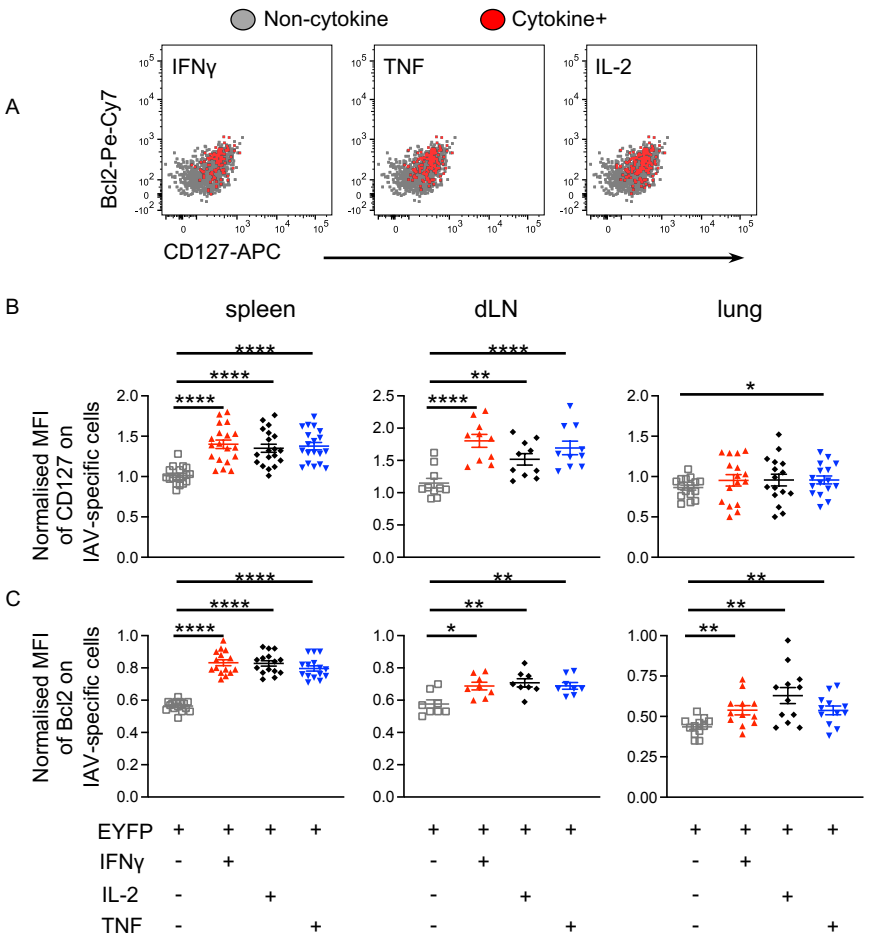

Figure 4: Triple cytokine+ CD4 and CD8 T cells are less likely to decline than single IFNγ+ T cells

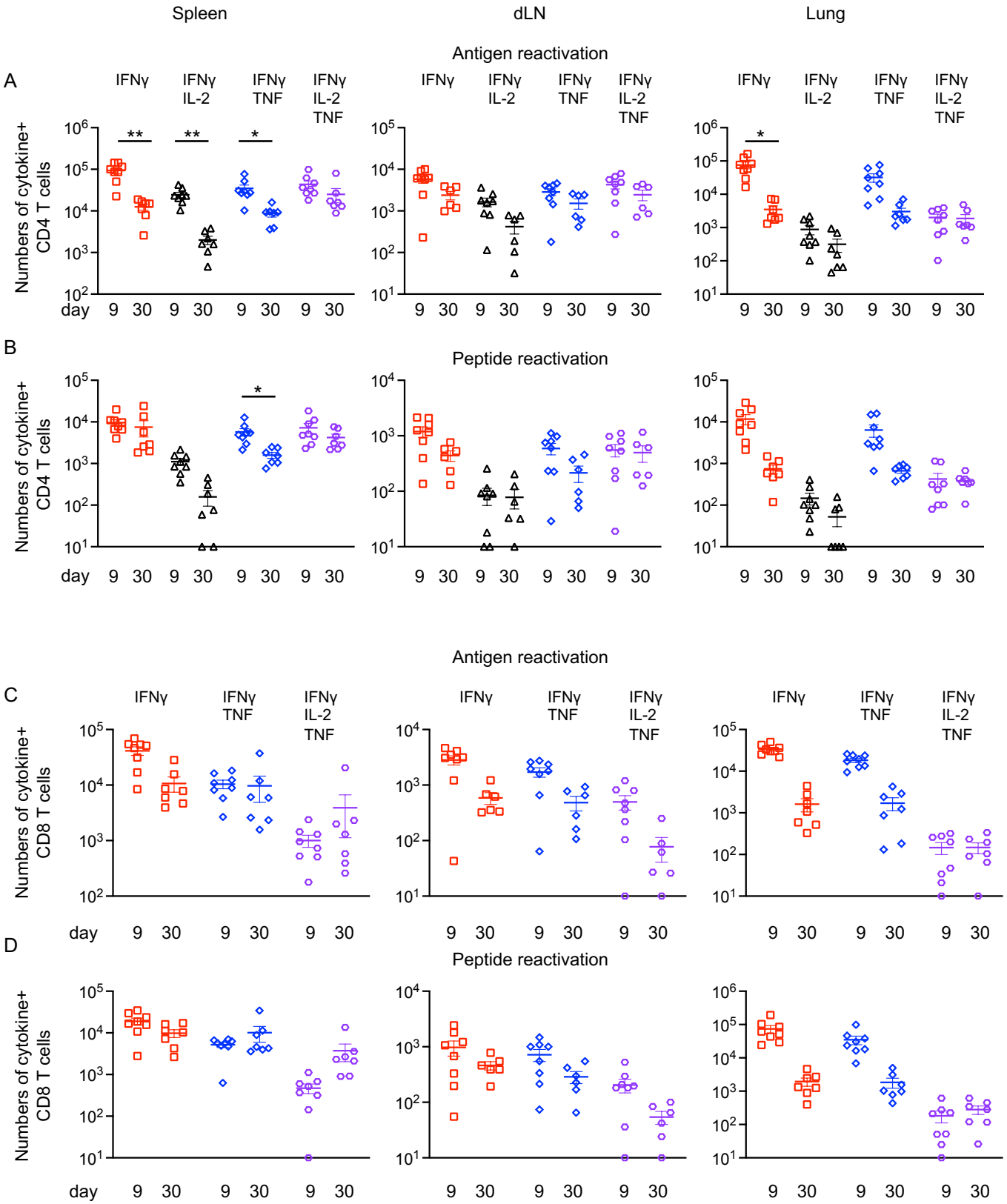

Figure 5: Triple cytokine+ T cells make more cytokine on a per cell basis than single cytokine+ T cells

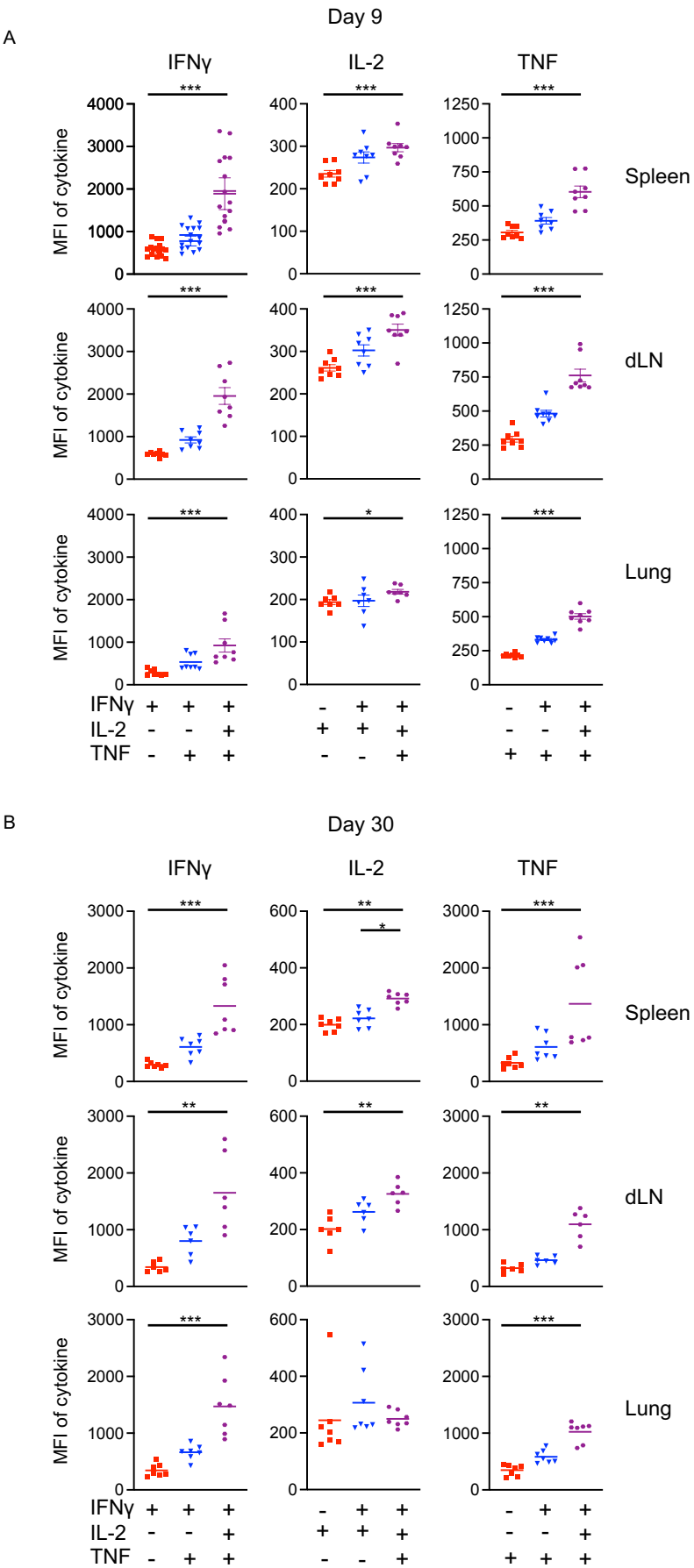

Figure 6: Single IFNγ+ CD4 and CD8 T cells are more likely to be in cell cycle 9 and 30 days after IAV infection than T cells producing multiple cytokines

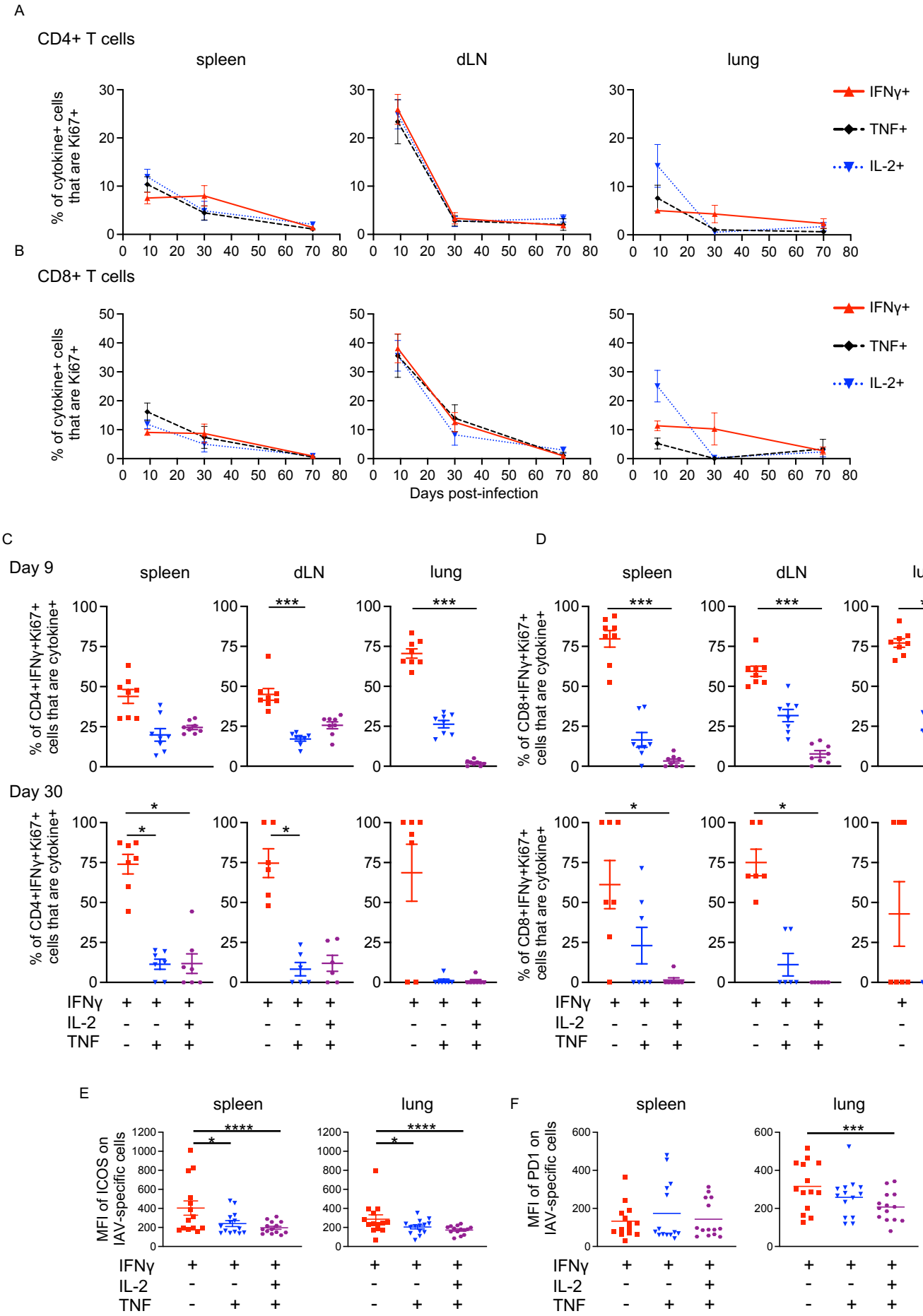

Figure 7: Triple cytokine+ CD4 T cells in the spleen express high levels of CD127 and Bcl2

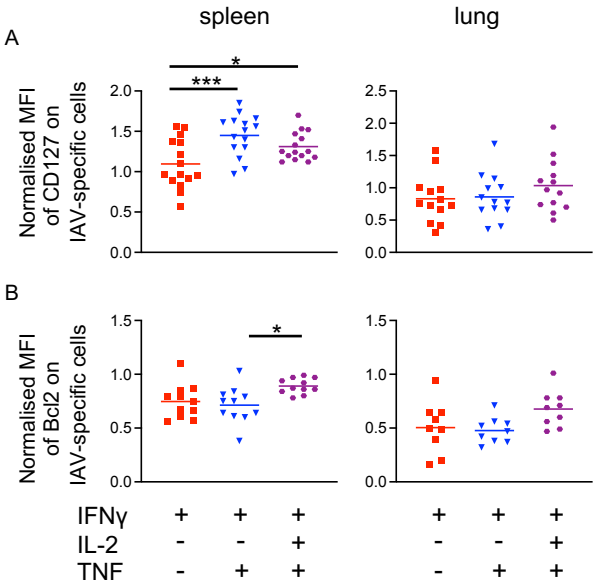

Figure 8: Triple cytokine+ CD4 T cells have a pro-survival transcriptional signature

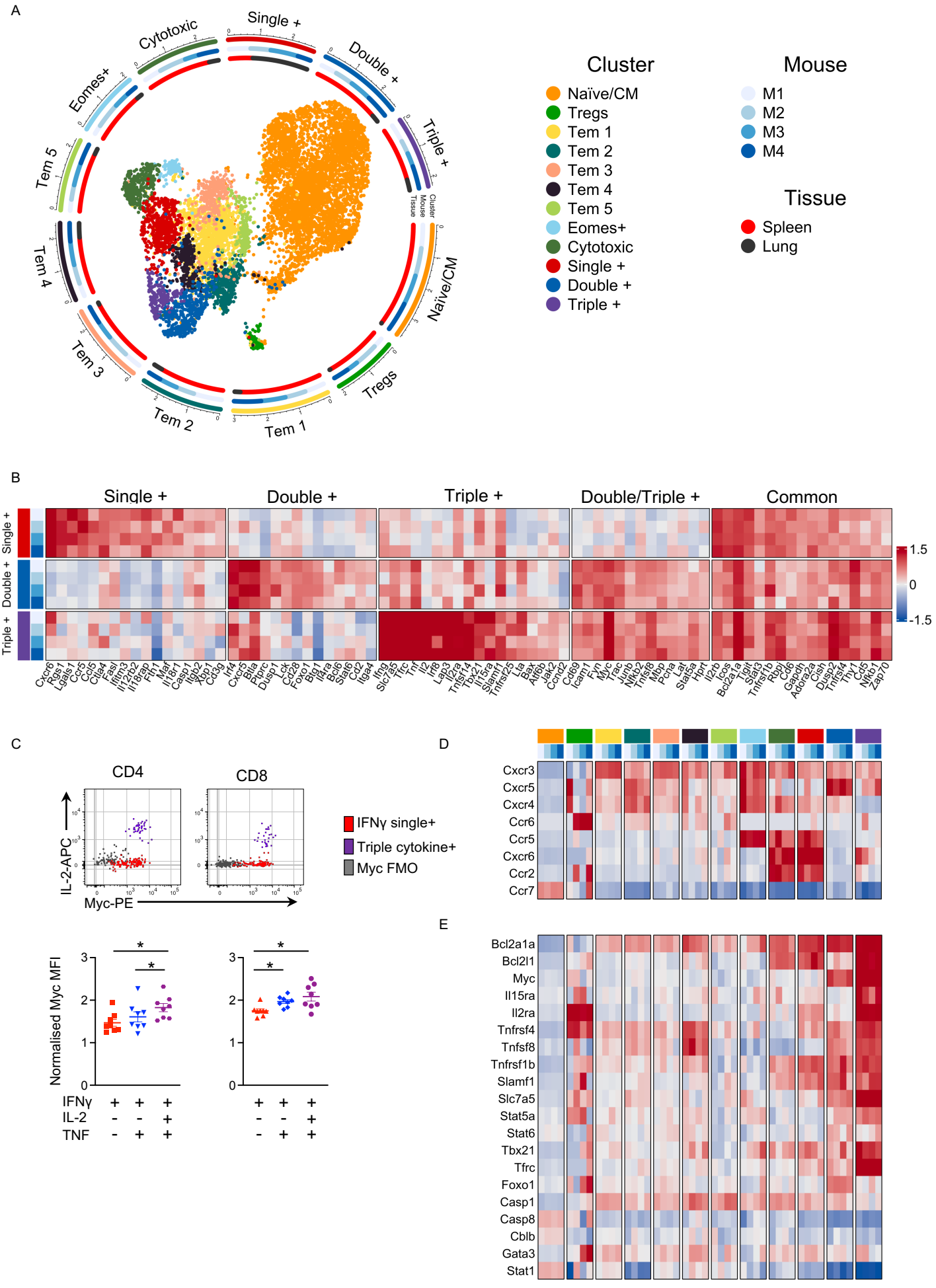

Figure 9: Identified TCR clones are found in all memory clusters

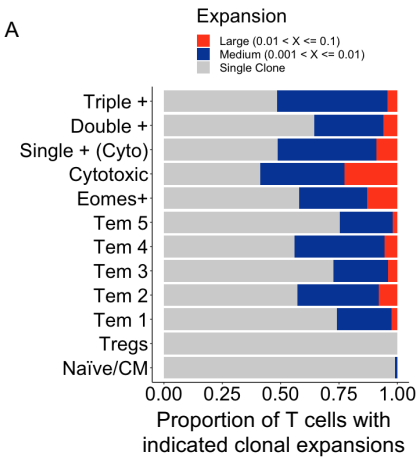

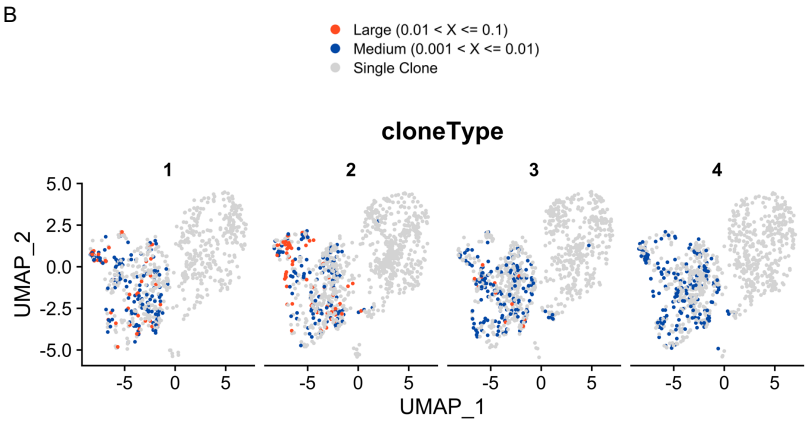

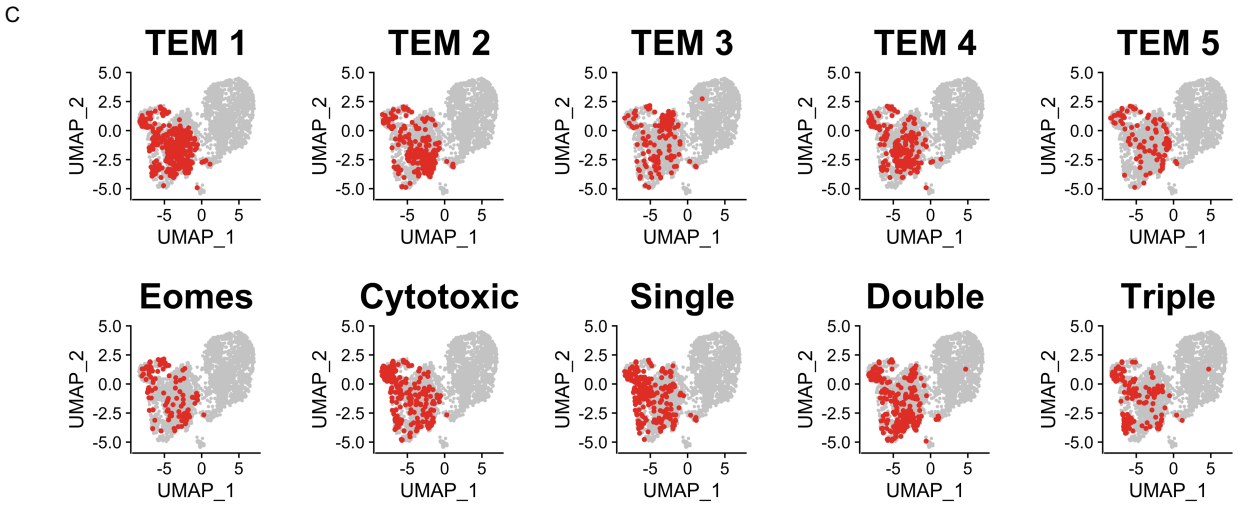

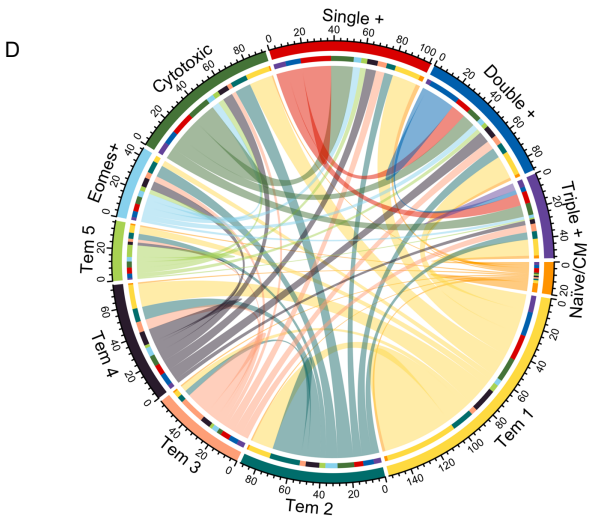

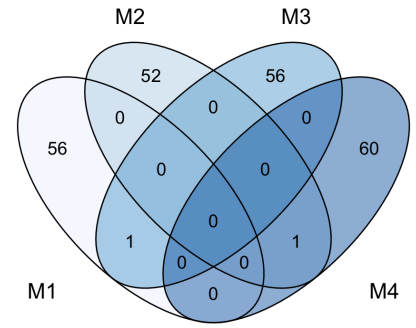

Figure 10: Triple cytokine+ are less likely to be in cell cycle than single IFNγ+ T cells following challenge infection